

Adenovirotherapy Delivering Cytokine and Checkpoint Inhibitor Augments CAR T Cells against Metastatic Head and Neck Cancer

Amanda Rosewell Shaw,^{1,2} Caroline E. Porter,^{1,2} Norihiro Watanabe,^{1,2} Kiyonori Tanoue,^{1,2} Andrew Sikora,⁴ Stephen Gottschalk,^{2,3} Malcolm K. Brenner,^{1,2,3} and Masataka Suzuki^{1,2}

¹Department of Medicine, Baylor College of Medicine, Houston, TX, USA; ²Center for Cell and Gene Therapy, Baylor College of Medicine, Texas Children's Hospital, Houston Methodist Hospital, Houston, TX, USA; ³Department of Pediatrics, Baylor College of Medicine, Houston, TX, USA; ⁴Department of Otolaryngology, Baylor College of Medicine, Houston, TX, USA

In solid tumors, chimeric antigen receptor (CAR)-modified T cells must overcome the challenges of the immunosuppressive tumor microenvironment. We hypothesized that pre-treating tumors with our binary oncolytic adenovirus (CAAd), which produces local oncolysis and expresses immunostimulatory molecules, would enhance the antitumor activity of HER2-specific CAR T cells, which alone are insufficient to cure solid tumors. We tested multiple cytokines in conjunction with PD-L1-blocking antibody and found that Ad-derived IL-12p70 prevents the loss of HER2.CAR-expressing T cells at the tumor site. Accordingly, we created a construct encoding the PD-L1-blocking antibody and IL-12p70 (CAAd_{12_PDL1}). In head and neck squamous cell carcinoma (HNSCC) xenograft models, combining local treatment with CAAd_{12_PDL1} and systemic HER2.CAR T cell infusion improved survival to >100 days compared with approximately 25 days with either approach alone. This combination also controlled both primary and metastasized tumors in an orthotopic model of HNSCC. Overall, our data show that CAAd_{12_PDL1} augments the anti-tumor effects of HER2.CAR T cells, thus controlling the growth of both primary and metastasized tumors.

INTRODUCTION

Solid tumors express a range of inhibitory cytokines¹ and immune checkpoint ligands² that impair the sustained activation and persistence of adoptively transferred chimeric antigen receptor (CAR)-expressing T cells. For optimal effector function, T cells require receptor activation (signal 1), co-stimulation (signal 2), and cytokine engagement (signal 3).³ Although CAR T cells can specifically target tumor antigens to receive signal 1 and contain embedded costimulatory sequences (signal 2), the immunosuppressive tumor microenvironment inhibits sustained activation of effector T cells by expressing immune checkpoint ligands that block co-stimulation (signal 2) and counteract pro-inflammatory cytokines (signal 3).¹

We have developed a system in which co-infection of an oncolytic adenovirus (Onc.Ad) with a helper-dependent Ad (HDAd) (combinatorial Ad vector [CAAd]) produces local oncolysis and expression

of multiple transgene products without loss of oncolytic titer.⁴ HDAd has a cargo capacity of up to 34 kb, and here we show that we can exploit the CAAd system to simultaneously disrupt the tumor microenvironment while producing checkpoint inhibitors (to augment signal 2) and stimulatory cytokines (to provide signal 3), thereby enabling adoptively transferred CAR T cells to target both local and metastatic disease. Local production of checkpoint inhibitors and stimulatory cytokines may have several advantages over systemic administration. Although checkpoint blockade with monoclonal antibodies has demonstrated success in multiple clinical trials,⁵ systemic administration of these antibodies has been associated with systemic adverse events and even with enhanced tumor growth.^{6,7} Likewise, many methods to provide exogenous signal 3 have been tested, including intravenous administration of pro-inflammatory recombinant cytokines (rCytokines) such as interleukin-2 (IL-2) or IL-15.⁸ However, there have been clinical toxicities associated with high circulating levels of rCytokines following their systemic administration.⁹

Head and neck squamous cell carcinomas (HNSCCs) are commonly locoregional diseases presenting at or near the body surface, making them amenable to direct intratumoral administration of Ad vectors.¹⁰ Although numerous clinical trials have demonstrated the safety and feasibility of Ad virotherapy for HNSCC, Ads alone are unable to cure bulky and metastatic disease. Additionally, although immune checkpoint ligands (e.g., PD-L1) and receptors (e.g., CTLA-4) have been identified on tumors in HNSCC patients,¹¹ a recent clinical trial showed that treatment with pembrolizumab (anti-PD-1 IgG) alone is insufficient to cure HNSCC, leading to questions about its clinical value in this setting.^{12,13}

Received 10 July 2017; accepted 8 September 2017;
<https://doi.org/10.1016/j.jmthe.2017.09.010>.

Correspondence: Masataka Suzuki, Department of Medicine, Center for Cell and Gene Therapy, Baylor College of Medicine, 1102 Bates Ave., Ste. 1770, Houston Texas 77030, USA.

E-mail: suzuki@bcm.edu

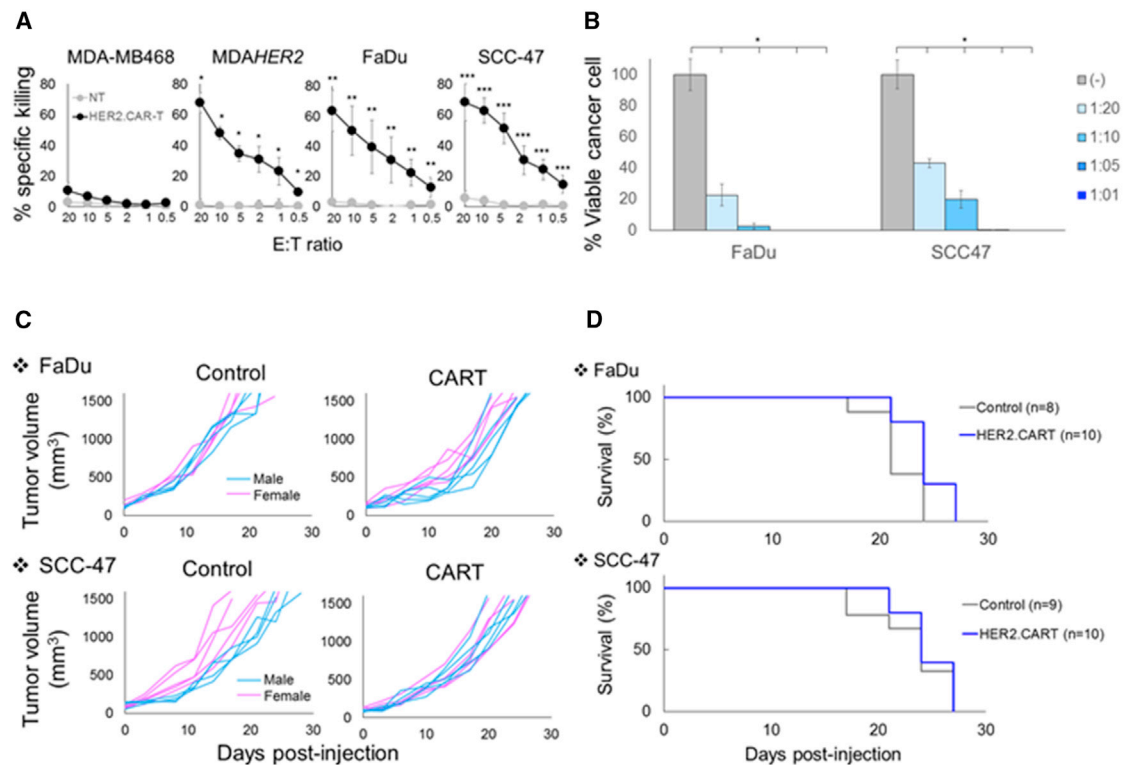


Figure 1. HNSCC Lines Resist HER2.CAR T Cells In Vivo

(A) The ability of HER2.CAR T cells to lyse HNSCC lines was assessed using a 4-hr ^{51}Cr release assay. Data are presented as means \pm SD ($n = 3$ donors). * $p < 0.002$, ** $p < 0.005$, *** $p < 0.001$. (B) FaDu and SCC-47 expressing *fluc* were cultured with increasing doses of HER2.CAR T cells. Viable cancer cells were analyzed at 120 hr by luciferase assay, and percent viability was calculated. Data are presented as means \pm SD ($n = 4$). * $p < 0.001$. (C) FaDu and SCC-47 cells were transplanted into the right flanks of NSG mice (pink, female; blue, male). A total of 1×10^6 HER2.CAR T cells were systemically administered after the tumor volume reached 100 mm^3 . Tumor volumes were measured at different time points. (D) Kaplan-Meier survival curve after administration of HER2.CAR T cells. The end point was established at a tumor volume of $>1,500 \text{ mm}^3$. Data are presented as means \pm SD ($n = 8-10$).

In this study, we show that local CAD treatment can simultaneously provide oncolysis, checkpoint inhibition, and a proinflammatory cytokine to head and neck tumors, thereby enhancing the antitumor efficacy of systemic CAR T cell therapy for HNSCC. We validated our combination approach using HER2.CAR T cells because these were recently reported to be safe in patients with osteosarcoma and glioblastoma^{14,15} and because recent preclinical and clinical data implicate HER2 as a therapeutic target in HNSCC with ongoing clinical trials of HER2-directed therapy.¹⁶ We demonstrate that the combination of CAD and HER2 CAR T cells produces anti-tumor activity even against otherwise resistant metastatic disease.

RESULTS

HNSCC Lines Resist Killing by HER2.CAR T Cells In Vivo

Over-activation of ErbB family receptors, including HER2, is one mechanism by which HNSCCs resist conventional treatment because increased HER2 expression is linked to worse prognosis, increased recurrence, and decreased survival in HNSCC patients.¹⁶ HNSCC is genetically classified into human papillomavirus (HPV)⁻ and HPV⁺ subclasses,¹⁷ and we found that both groups express HER2 (Figure S1). To discover whether HER2 expression on HNSCCs

was sufficient for recognition and killing by CAR T cells, we co-cultured HNSCC lines with T cells expressing a second-generation HER2-specific CAR with CD28, ζ -signaling domains (HER2.CAR T cells^{14,15}). We evaluated the short-term (4-hr Cr release assay) and long-term (5-day co-culture) cytotoxicities of these HER2.CAR T cells to FaDu (HPV⁻) and SCC-47 (HPV⁺) (Figures 1A and 1B). We confirmed that HER2.CAR T cells had a dose-dependent killing effect in both assays, indicating that HNSCC lines express sufficient levels of HER2 for HER2.CAR T cell recognition and killing.

We showed that, in the absence of tumor, 1×10^6 HER2.CAR T cells expanded minimally in NOD.Cg-Prkdc^{scid}/IL2rg^{tm1Wjl}/Sz (NSG) mice after systemic injection (Figure S2) and did not produce xenogeneic graft versus host disease, an effect that may confound the assessment of specific anti-tumor activity. We next evaluated the anti-tumor efficacy of HER2.CAR T cells by subcutaneously transplanting FaDu or SCC-47 tumor cells. After the tumor volume reached 100 mm^3 , we injected 1×10^6 HER2.CAR T cells systemically and followed the tumor volume (Figure 1C). Although HER2.CAR T cells effectively killed the HNSCC lines in vitro, they had minimal anti-tumor effects and no benefit to survival in vivo (Figure 1D). These

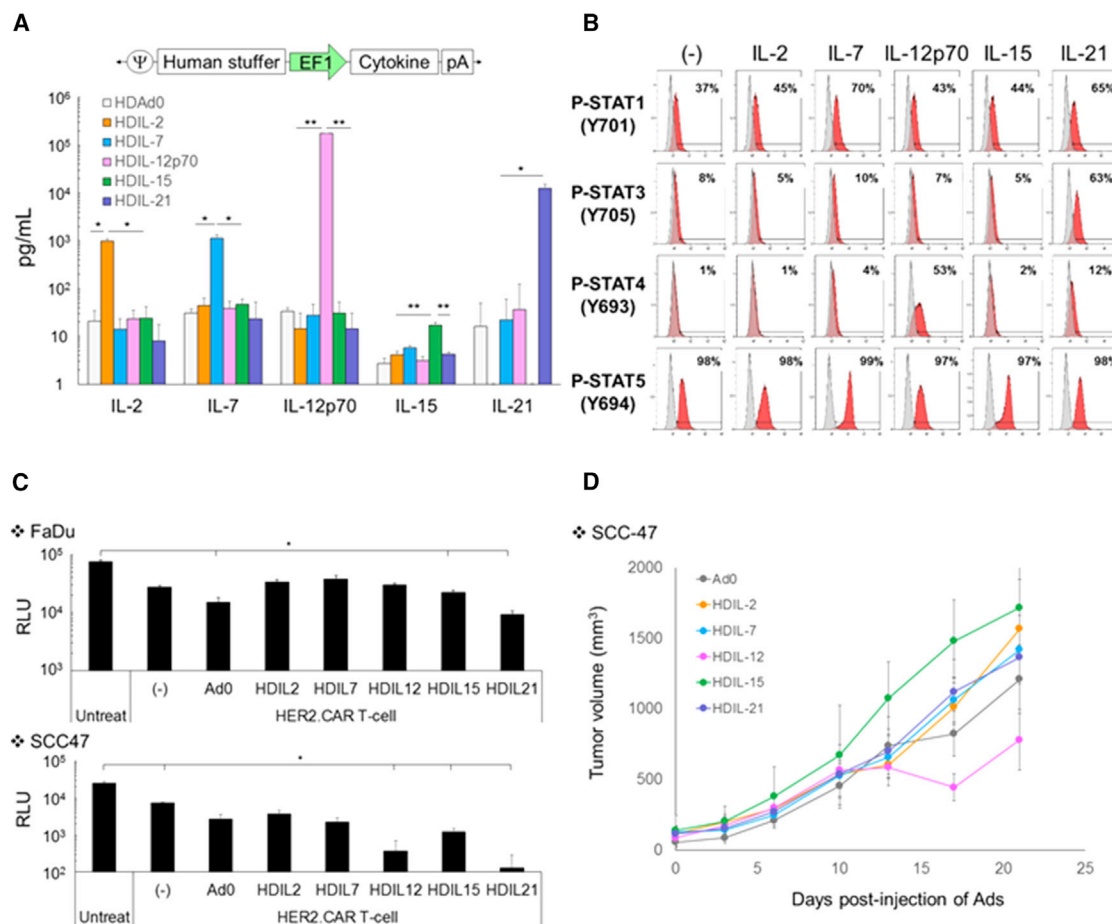


Figure 2. HDAd-Derived Cytokines Minimally Enhance the Anti-tumor Effect of HER2.CAR T Cells In Vitro and In Vivo

(A) Schematic structure of HDAd encoding a cytokine expression cassette (HDAdCyto). A549 cells were infected with 100 vps/cell of HDAdCyto. Media were collected 48 hr post-infection, and cytokine levels in the media were measured by ELISA. Data are presented as means \pm SD (n = 4). *p < 0.05, **p < 0.001. (B) HER2.CAR T cells expanded with IL-2 were cultured in the presence of 10 ng/mL recombinant cytokines for 30 min, and phosphorylation of STATs was analyzed by flow cytometry. The experiments were repeated with HER2.CAR T cells derived from a second donor with similar results. (C) FaDu or SCC-47 expressing *flLuc* cells were infected with 100 vps/cell of HDAdCyto. HER2.CAR T cells were added 24 hr post-infection (effector:target ratio of 1:40). Cells were harvested 120 hr post-co-culture, and viable cancer cells were analyzed by luciferase assay. Data are presented as means \pm SD (n = 4). *p < 0.001. (D) SCC-47 cells were transplanted into the right flanks of NSG female mice. A total of 1×10^8 vps of HDAdCyto were injected intra-tumorally. A total of 1×10^6 HER2.CAR T cells were systemically administered 3 days post-injection of HDAd, and tumor volumes were measured at different time points. Data are presented as means \pm SD (n = 3).

results suggest that additional immunomodulation is required to enhance the anti-tumor effect of HER2.CAR T cells in vivo.

HDAd-Derived Cytokines Minimally Enhance the Anti-tumor Effect of HER2.CAR T Cells In Vitro and In Vivo

Although co-expressing a cytokine with CAR has been shown to enhance the anti-tumor effects of CAR T cells (“armored” CAR T cells) in vivo,^{18,19} constitutive and systemic cytokine expression by expanded armored CAR T cells may cause off-target toxicity. To address whether local provision of cytokine at the tumor site similarly enhances anti-tumor activity of CAR T cells, we generated HDAd²⁰ expressing IL-2, IL-7, IL-12p70, IL-15, or IL-21 (HDAdCyto) to exogenously provide local cytokine to HER2.CAR T cells.

We first confirmed that the HDAd expressed the encoded cytokine in vitro (Figure 2A). We also confirmed that the expanded HER2.CAR T cells used in the experiments responded to these cytokines and phosphorylated signal transducers and activators of transcription (STATs) (Figure 2B). IL-7, IL-12p70, IL-15, and IL-21 specifically phosphorylated the appropriate STATs of HER2.CAR T cells (IL-7 and IL-15, STAT5; IL-12p70, STAT4; IL-21, STAT3), indicating that HER2.CAR T cells respond as anticipated to these cytokines.^{21,22} Of note, HER2.CAR T cells had no additional STAT5 phosphorylation in the presence of IL-2. Because we expanded HER2.CAR T cells with recombinant human IL-2, IL-2-dependent STAT5 phosphorylation may already have been at maximum levels.

We then determined which HDAd $Cyto$ enhanced HER2.CAR T cell killing in vitro (Figure 2C). Although HDAd $Cyto$ did not improve HER2.CAR T cell killing of FaDu in co-culture, IL-12p70, IL-15, and IL-21 consistently and significantly ($p < 0.001$) improved the anti-tumor effects of HER2.CAR T cells co-cultured with SCC-47 (Figure 2C). To confirm that local IL-12p70, IL-15, or IL-21 expression improves the anti-tumor activity of HER2.CAR T cells in vivo, we evaluated the anti-tumor effects of HDAd $Cyto$ and HER2.CAR T cells in an SCC-47 xenograft mouse model (Figure 2D). We found that only HDIL-12 improved the anti-tumor effects of HER2.CAR T cells compared with mice treated with control HDAd (Ad0) in vivo. However, the improvement of HER2.CAR T cell activity by IL-12 in vivo was modest, implying that increased local provision of cytokine (signal 3) alone may be insufficient to produce durable responses against HNSCC tumors.

HDAd-Derived IL-12p70- and PD-L1-Blocking Antibody Maintains HER2.CAR Expression of Adoptively Transferred HER2.CAR T Cells In Vivo

We next repeated the co-culture experiments in the presence of HDAd-expressing PD-L1-blocking antibody (HDAd $PDL1^7$) and HDAd $Cyto$ because both FaDu and SCC-47 upregulate PD-L1 in the presence of interferon γ (IFN γ) produced by effector T cells (Figure S3A). We found that, in conjunction with PD-L1-blocking antibody, IL-12p70 and IL-21 dramatically improved HER2.CAR T cell killing in SCC-47 co-culture (Figure S3B), indicating that the additive anti-tumor effects of cytokine (signal 3) are enhanced by blockade of the PD-1:PD-L1 interaction (to augment signal 2).

To determine whether cytokine and PD-L1-blocking antibody together enhanced the anti-tumor activity of HER2.CAR T cell in vivo, we screened HDAd $Cyto$ and HDAd $PD-L1$ in FaDu (HPV $^-$) and SCC-47 (HPV $^+$) xenograft mouse models. We found that the combination of HDAdIL-12p70 with HDAd $PD-L1$ significantly improved the anti-tumor effects of adoptively transferred HER2.CAR T cells in both FaDu and SCC-47 xenograft models (Figure 3A).

To address how HDAd derived IL-12p70 enhanced HER2.CAR T cell activity in vivo, we first measured the expansion of firefly luciferase ($ffLuc$)-labeled HER2.CAR T cells at tumor sites (Figure 3B). We found that $ffLuc$ activity was identical irrespective of treatment group in both FaDu and SCC-47 xenograft models, suggesting that $ffLuc$ -transduced T cells expand and persist at tumor sites at a similar level regardless of the treatment group. When we phenotyped HER2.CAR T cells from the tumor sites 22 days following adoptive transfer (Figure 3C), however, we found that HER2.CAR T cells from tumor sites treated with HDAdIL-12p70 maintained pre-infusion levels of HER2.CAR expression at 70%–90%. In contrast, HER2.CAR positivity decreased from 90% (pre-infusion; Figure S4A) to 20% in HER2.CAR T cells from tumors treated with any other HDAd $Cyto$. There were only minor (and statistically non-significant) differences in the CD4 and CD8 ratio, memory phenotype, and PD-1, LAG3, or TIM3 expression levels of HER2.CAR T cells between the HDAd $Cyto$ conditions (Figure S4B). We next isolated HER2.CAR T cells from FaDu and SCC-47 tumors 22 days post-infusion and extracted

DNA and RNA from these T cells to quantify the HER2.CAR copy number at the DNA and RNA levels (Figure 3D). Only HER2.CAR T cells from tumor sites treated with HDAdIL-12p70 maintained HER2.CAR copy numbers at their pre-injection levels. Hence, HDAd-derived IL-12p70 sustains the presence of HER2.CAR-encoding and -expressing T cells at tumor sites, thus maintaining the anti-tumor effects of HER2.CAR T cells in vivo.

Benefits of Combining Helper-Dependent and Onc.Ads (CAAd)

Having identified the optimal cytokine and checkpoint components of the HDAd vector, we constructed a single HDAd encoding both IL-12p70 and PD-L1-blocking antibody expression cassettes (HDAd $I2_PDL1$) and confirmed that it expressed both transgenes at levels similar to HDAd expressing a single transgene (Figure 4A). One drawback of the HDAd system, however, is that it lacks the ability to replicate and destroy infected cancer cells (oncolysis). Because we have previously shown that tumor cells co-infected with Onc.Ad and HDAd (CAAd) replicate both Onc.Ad and HDAd,^{4,7} we hypothesized that combining HDAd $I2_PDL1$ with Onc.Ad would lead to cycles of production and release of both the oncolytic and the immunogenic components (IL-12p70 and PD-L1-blocking antibody).

First we tested the antitumor efficacy of Onc.Ad5/3 Δ 24 because this oncolytic virus has been clinically tested in patients with solid tumors, including HNSCC.²³ We injected the virus locally into both FaDu and SCC-47 xenograft models and found that it had minimal anti-tumor effects (Figure S5), suggesting that, like CAR T cells, oncolysis alone is insufficient to cure bulky HNSCCs. Next we confirmed that co-infection of Onc.Ad with HDAdIL12_PDL1 (CAAd $I2_PDL1$; Onc.Ad:HDAd = 1:10⁴) amplified IL-12p70 and PD-L1-blocking antibody expression in co-infected FaDu and SCC-47 cells in vitro (Figure 4B). To test whether increased transgene expression was dependent on the amplification of HDAd vector DNA, we quantified both HDAd and Onc.Ad vector copies using primer sets for each backbone (Table S1) 48 hr post-infection (Figure 4C). Cells infected with CAAd $I2_PDL1$ had 100-fold more HDAd vector copies than cells infected with HDAd alone. To verify whether CAAd $I2_PDL1$ induces both the amplification of HDAd and the lytic effects of Onc.Ad, cellular lysis of CAAd $I2_PDL1$ was evaluated using an MTS cell proliferation assay 96 hr post-infection (Figure 4D). CAAd $I2_PDL1$ had dose-dependent lytic effects in infected FaDu and SCC-47 cell lines, although it was not as potent as Onc.Ad alone, likely because the ratio of Onc.Ad to HDAd in the CAAdVEC treatment was just 1:10.^{4,7}

Benefits of Combining CAAd and CAR T Cells In Vivo

We evaluated the anti-tumor effects of combinatorial treatment with CAAd $I2_PDL1$ and HER2.CAR T cells in FaDu and SCC-47 xenograft models (Figure 5A). Combinatorial treatments with HER2.CAR T cells and Onc.Ad, CAAd $I2$, or CAAd $PDL1$ were used as controls. CAAd $I2_PDL1$ and HER2.CAR T cells significantly extended the median survival of mice from 21 days (FaDu, no treatment) or 24 days (SCC-47, no treatment) to more than 100 days (Figure 5B; Table 1). Combinatorial treatment with CAAd $I2_PDL1$ and HER2.CAR T cells also significantly extended the median survival compared with mice

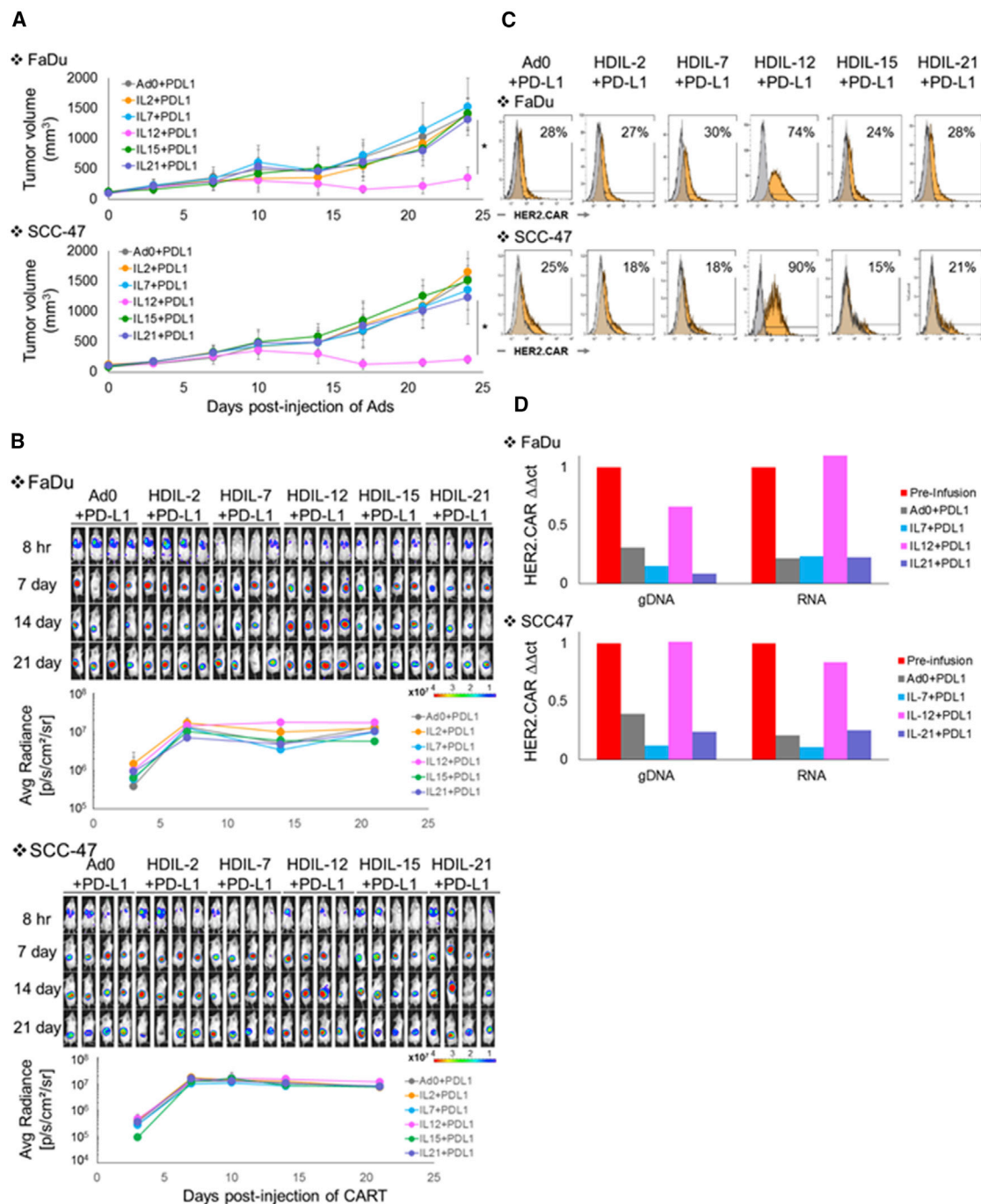


Figure 3. HDAd-Derived IL-12p70 and PD-L1-Blocking Antibody Increase the Anti-tumor Efficacy of Adoptively Transferred HER2.CAR T Cells In Vivo

FaDu or SCC-47 cells were transplanted into the right flanks of NSG mice. A total of 1×10^8 vps of HDAdCyto and HDAdPDL1 (1:1) were injected intra-tumorally. A total of 1×10^6 HER2.CAR T cells expressing firefly luciferase (ffLuc) were systemically administered 3 days post-injection of HDAds. (A) Tumor volumes were measured at different time points. Data are presented as means \pm SD ($n = 4$). * $p < 0.001$. (B) Bioluminescence of HER2.CAR T cells was monitored at different time points. Data are presented as means \pm SD ($n = 4$). (C) T cells at the tumor site were isolated 22 days post-injection, and HER2.CAR levels on T cells were analyzed by flow cytometry. The experiments were repeated with similar results. (D) T cells from tumor sites treated with HDAd0, HDAdIL-7, HDAdIL-12, or HDAdIL-21 co-injected with HDAdPDL1 were isolated 22 days post-injection and purified by a CD3 MACS column. To achieve sufficient T cells for analysis, cells from each group were pooled before analysis. DNA and RNA were extracted from purified T cells, and HER2.CAR copy numbers at DNA and RNA levels in each sample were quantified. The experiments were repeated with similar results.

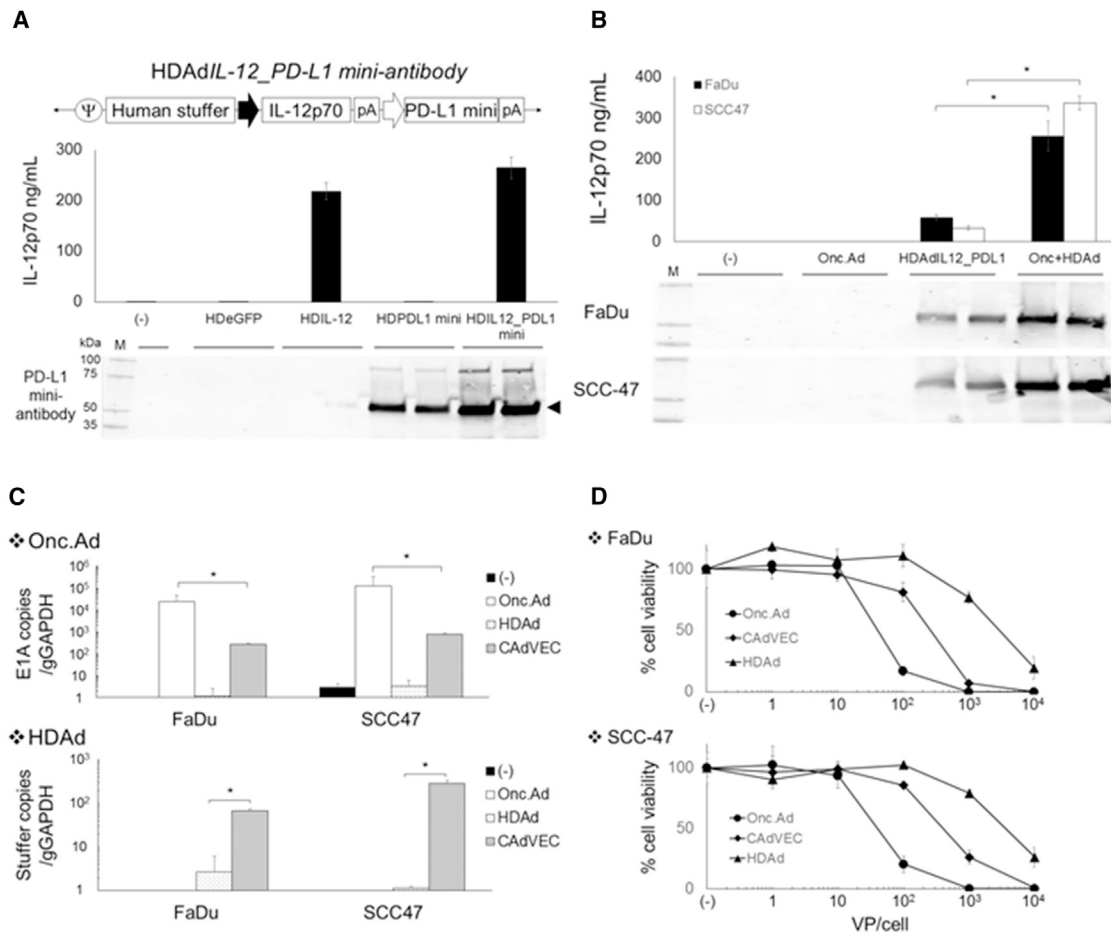


Figure 4. Co-infection of Onc.Ad with HDAd Expressing Both IL-12p70 and PD-L1 Mini-Antibody Amplifies IL-12p70 and PD-L1-Blocking Antibody Expression with Oncolysis In Vitro

(A) Schematic structure of HDAd encoding human IL-12p70 and anti-PD-L1 mini-antibody expression cassettes (HDAdIL12_PDL1). A549 cells were infected with 100 vps/cell of HDAdEGFP, HDAdIL-12, HDAdPD-L1, or HDAdIL12_PDL1. Media were collected 48 hr post-infection. Medium samples were subjected to IL-12p70 ELISA and western blotting for PD-L1 mini-antibody, which was detected by anti-HA antibody. (B) FaDu and SCC-47 cells were infected with a total of 10 vps/cell of HDAdIL12_PDL1 or Onc.Ad or with CAAd12_PDL1 (Onc.Ad:HDAd, 1:10). Medium samples were collected 48 hr post-infection. The levels of IL-12p70 and PD-L1 mini-antibody in medium samples were quantified by IL-12p70 ELISA assay and western blotting for PD-L1 mini-antibody, respectively. Data are presented as means \pm SD (n = 4). *p < 0.001. (C) DNA samples were extracted 48 hr post-infection, and Onc.Ad and HDAd vector copy numbers were measured by qPCR. Data were normalized with human genomic GAPDH. Data are presented as means \pm SD (n = 4). *p = 0.008. CAAdVEC: Onc.Ad:HDAdIL12_PDL1, 1:10. (D) FaDu and SCC-47 cells were infected with increasing doses of HDAdIL12_PDL1 or Onc.Ad or with CAAdVEC (Onc.Ad: HDAdIL12_PDL1, 1:10). Viable cells were analyzed at 96 hr by MTS assay. Data are presented as means \pm SD (n = 6).

treated with HER2.CAR T cells and Onc.Ad (oncolysis), HER2.CAR T cells and CAAd12 (oncolysis + IL-12p70), or HER2.CAR T cells and CAAdPDL1 (oncolysis + PD-L1-blocking antibody) in both animal models, indicating that all components (oncolysis, IL-12p70, and PD-L1-blocking antibody) are required to maximize the anti-tumor effects of HER2.CAR T cells. HER2.CAR T cells were detected at tumor sites for more than 100 days in surviving mice (Figure 5C; Figure S6) and maintained their HER2.CAR expression (Figure S7). IFN γ and IL-12p70 were also detected in the blood of surviving mice (Figure 5D). These results indicate that, in the presence of the combination of oncolysis, IL-12p70, and PD-L1-blocking antibody, HER2.CAR T cells persist long-term and that their continued transgene expression at the tumor sites correspondingly prolonged control

of tumor growth. Mice treated with these combined therapies had no weight loss or other visible adverse events (Figure S8), suggesting that the treatments, including the oncolysis and transgene products, had minimal toxicity in mice.

Combination of CAAd12_PDL1 and HER2.CAR T Cells Controls Both Primary and Metastasized HNSCC Tumors in an Orthotopic Mouse Model

Nearly 50% of HNSCC patients have lymphatic metastasis, contributing to continued poor disease prognosis.²⁴ To address whether CAAd12_PDL1 treatment at the primary tumor site can augment the anti-tumor effects of systemically administered HER2.CAR T cells and control the growth of both primary and metastasized tumors,

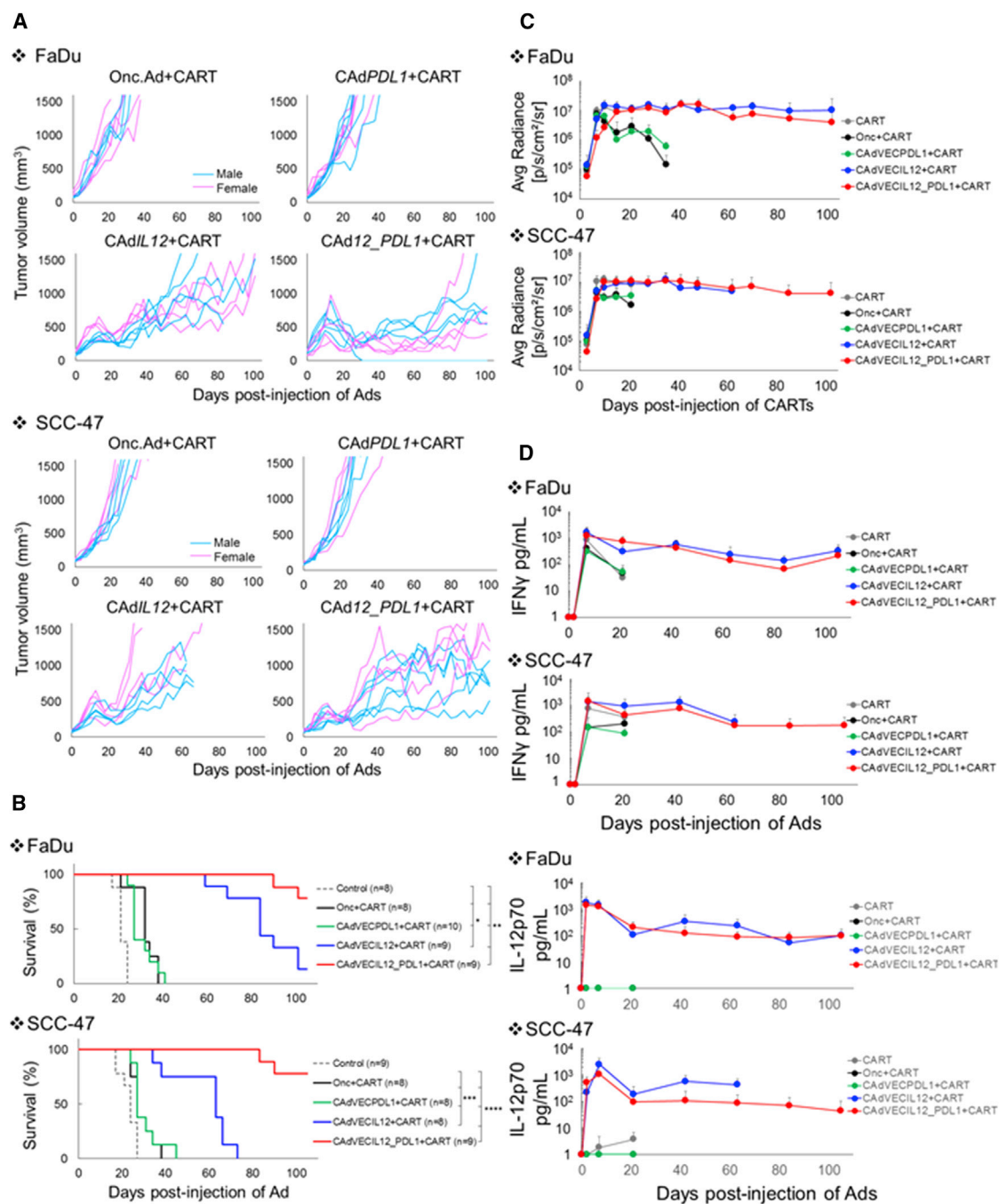


Figure 5. CAd12_PDL1 Enhances the Anti-tumor Effects of HER2.CAR T Cells In Vivo

FaDu or SCC-47 cells were transplanted into the right flanks of NSG mice (pink, female; blue, male). A total of 1×10^5 vps of Onc.Ad, CAdPDL1, CAdIL-12, or CAd12_PDL1 (Onc:HD, 1:20) were injected intra-tumorally. A total of 1×10^6 HER2.CAR T cells expressing *flLuc* were systemically administered 3 days after injection of Ads. (A) Tumor volumes were measured at different time points. (B) Kaplan-Meier survival curve after administration of Ad gene therapy. The end point was established as a tumor volume of $>1,500$ mm³. Data are presented as means \pm SD (n = 8–10). *p < 0.003, **p < 0.007, ***p < 0.01, and ****p < 0.001. (C) The bioluminescence of HER2.CAR T cells was monitored at different time points. Data are presented as means \pm SD (n = 8–10). (D) Serum samples were collected at 0, 3, 10, 24, 45, 66, 87, and 108 days after injection of Ads, and IFN γ and IL-12p70 levels in serum were measured by ELISA. Data are presented as means \pm SD (n = 8–10).

Table 1. Median Survival of Animals

	Control	Onc.Ad + CART	CAdPDL1 + CART	CAd 12 + CART	Cad 12 _ PDL1 + CART
FaDu	21 days	32 days	27 days	84 days	>105 days
SCC-47	24 days	27 days	27 days	63 days	>105 days

CART, chimeric antigen receptor T cell.

we evaluated the anti-tumor effects of combinatorial treatment in an orthotopic HNSCC model that produces lymph node (LN) metastases (Figure S9A).^{17,25,26} We transplanted FaDu into the tongues of NSG mice, and 6 days later injected 1×10^8 viral particles (vps) of CAd12_PDL1 into the tongue. Three days after CAd12_PDL1 treatment, we injected 1×10^6 *ffLuc*-labeled HER2.CAR T cells intravenously (i.v.) (Figure 6A) and monitored the distribution of HER2.CAR T cells (Figure 6B). HER2.CAR T cells infiltrated both primary and metastasized tumors by 3 days post-injection in the presence and absence of CAd treatment, indicating that HER2.CAR T cells can target both primary and metastasized tumors independent of CAd. Although T cell signals persisted at tumor sites in mice treated with HER2.CAR T cells alone, similarly to mice who also received a CAd12_PDL1 injection (Figure 6B), all mice receiving HER2 CAR T cells alone were terminated by day 60 because of weight loss. In contrast, there was no weight loss because of tumor growth in mice treated with combinatorial treatment (Figure S10). These results suggest that CAd-derived transgenes at the primary tumor can promote the activation of adoptively transferred HER2.CAR T cells, which can then control the growth of both primary and metastasized tumors.

To address how each component of combinatorial treatment controls primary and metastasized tumor growth, we next transplanted FaDu labeled with *ffLuc* into the tongues of NSG mice and monitored tumor growth by *ffLuc* activity (Figure 6C). Mice were treated with a single agent or a combination. Mice treated with both CAR T cells and CAd had significantly reduced *ffLuc* activity at primary and metastasized tumors 10 days post-CAd injection compared with control animals and with those receiving single-agent treatments. Dual treatment also extended the median survival from 13 days (untreated group) to more than 100 days (Figure 6D), and these mice showed control at both primary and metastatic sites. HER2.CAR T cells were detected at both tumor sites 120 days post-infusion and maintained their HER2.CAR expression (Figure 6E). Notably, both Onc.Ad and HDAd vector DNAs were detected in primary tumors (tongue) of mice receiving CAd12_PDL1 but were undetectable in the LN area (Figure S9B), suggesting that the HER2.CAR T cells, unlike locally injected CAd, play a major role in the control of LN metastases and that CAd-derived immunostimulatory transgene expression is required for these HER2.CAR T cells to control LN metastases.

DISCUSSION

Here we demonstrate that CAd12_PDL1 augments the anti-tumor effects of adoptively transferred HER2.CAR T cells HNSCC xenograft

and orthotopic mouse models, leading to control of both bulky (xenograft) and metastasized (orthotopic) tumor growth.

To date, local Onc.Ad treatment has been unable to eradicate tumors in HNSCC patients because locally injected Ads have limited distribution to metastasized tumors.¹⁰ In contrast, CAR T cells can home to both primary and metastasized tumors, potentially overcoming the limited systemic anti-tumor effects of locally administered Ad-based cancer immunotherapies. But although both Onc.Ad5/3Δ24²³ and HER2.CAR T cells^{14,15} effectively kill HNSCC lines in vitro, neither treatment had substantial anti-tumor effects on HNSCC tumors in vivo when used alone or in combination, consistent with their limited activity in clinical trials.

Compared with B cell malignancies, solid tumors, including HNSCCs, pose unique challenges for CAR T cell therapy because they express a range of inhibitory cytokines and immune checkpoint ligands such as PD-L1.¹ We thus developed a binary Onc.Ad system in which a single package of an Onc.Ad with HDAd (CAd or CAdVEC) produces local oncolysis and expresses multiple transgene products without loss of oncolytic titer.⁴ HDAd has a cargo capacity of up to 34 kb and therefore can express multiple immunomodulatory molecules in a single vector, and co-infected Onc.Ad replicates both Onc.Ad and HDAd. We demonstrated that local CAd expressing PD-L1-blocking antibody (CAdPDL1) can boost the anti-tumor activity of adoptively transferred HER2.CAR T cells compared with treatment with either treatment alone in prostate and cervical carcinoma xenograft models;⁷ however, we found this approach to be insufficient for HNSCC xenograft tumors.

Several cytokines, including IL-7, IL-15, and IL-21, maintain the memory phenotype of CAR T cells when used for ex vivo expansion or given to mice in conjunction with CAR T cells. These effects are mediated by phosphorylation of STAT proteins, including STAT5 and STAT3.^{21,27–29} Thus, we hypothesized that adding an HDAd expressing a cytokine to provide signal 3 (HDAdCyto) to our CAdPDL1 (which augments signal 2) would further enhance HER2.CAR T cell activity locally and precipitate superior systemic CAR T cell killing. 22 days post-injection, all cytokines tested (IL-2, IL-7, IL-12p70, IL-15, and IL-21) showed similar effects on T cell proliferation, memory phenotype, and exhaustion marker expression. However, in vivo, IL-12p70 best augmented the antitumor activity of HER2.CAR T cells in the presence of PD-L1-blocking antibody, and only IL-12p70 prevented the loss of CAR encoding and expressing T cells at tumor sites, indicating that maintenance of CAR expression likely contributes to increased in vivo tumor killing in the presence of IL-12p70. Of the cytokines tested in this study, only IL-12p70 phosphorylates STAT4, suggesting that STAT4 may be a key signaling pathway in HER2.CAR T cell activation and/or attenuation of epigenetic silencing of HER2.CAR genes encoded in HER2.CAR T cells in vivo. Because IL-12p70 polarizes naive T cells toward the T_H1 subset in the presence of IFN γ ,³⁰ which is produced by CAR T cells, additional polarization of HER2.CAR T cells toward the T_H1 subset or maintenance of the T_H1 subset at the tumor site may contribute to

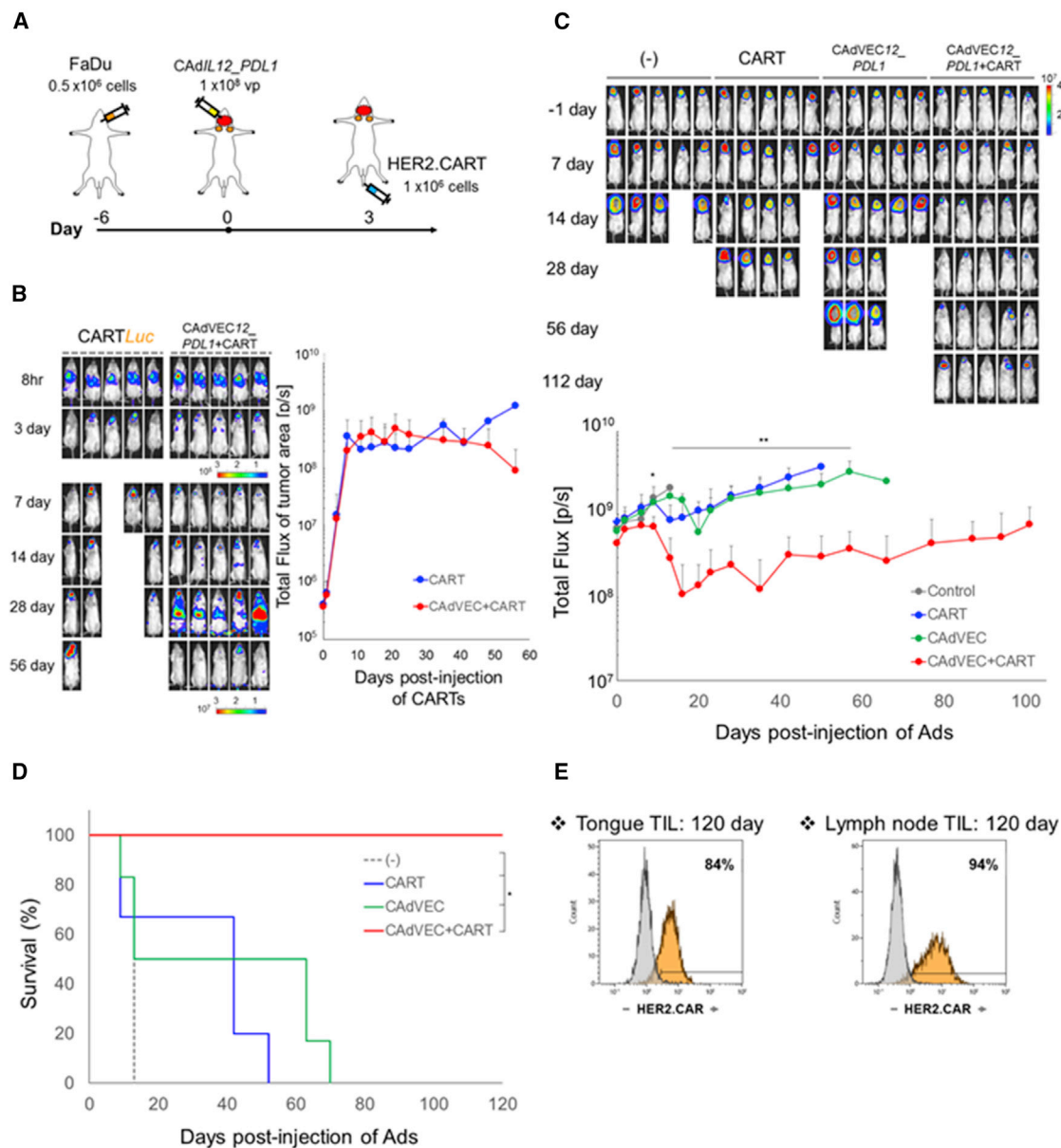


Figure 6. Combinatorial Treatment Can Control Both Primary and Metastasized Tumors in an Orthotopic HNSCC Model

(A) Schematic flow of HNSCC orthotopic animal experiment. (B) FaDu cells were transplanted into the tongues of NSG mice. A total of 1×10^6 vps of CAd12_PDL1 (Onc:HD, 1:20) were injected into the tongues. A total of 1×10^6 HER2.CAR T cells expressing *flLuc* were systemically administered 3 days after injection of CAd. The bioluminescence of HER2.CAR T cells at the tumor area was monitored at different time points. Data are presented as means \pm SD ($n = 5$). (C) FaDu cells expressing *flLuc* were transplanted into the tongues of NSG mice. A total of 1×10^8 vps of CAd12_PDL1 (Onc:HD, 1:20) were injected into the tongue. A total of 1×10^6 HER2.CAR T cells were systemically administered 3 days after injection of CAd. Bioluminescence of FaDu cells was monitored at different time points. Data are presented as means \pm SD ($n = 6-8$). * $p = 0.017$, ** $p < 0.005$. (D) Kaplan-Meier survival curve after administration of Ad gene therapy. The end point was established as an animal body weight $< 80\%$. Data are presented as means \pm SD ($n = 6-8$). * $p < 0.003$. (E) T cells were isolated from tongue and lymph node sites 120 days post-infusion, and HER2.CAR expression was analyzed by flow cytometry.

anti-tumor activity. Clinical trials with recombinant IL-12 for patients with advanced cancers revealed a modest clinical response and severe toxicity when high doses (500 ng/kg) were used.³¹ The serum concentration of recombinant IL-12 over a 24-hr period

ranged from approximately 10 ng/mL to 2 ng/mL.³¹ Because CAd12_PDL1-derived IL-12 is produced and concentrated at the tumor site, this results in low level blood concentrations (0.1 ng/mL).^{4,32} We have previously demonstrated such benefits for local CAd

production of anti-PD-L1 immunoglobulin G (IgG),⁷ suggesting that intratumoral CAD treatment can provide the benefits of systemic recombinant cytokine and antibody treatments while minimizing their associated toxicities.

Because lymphatic metastases contribute to the poor disease prognosis of HNSCC patients,²⁴ we used an orthotopic model with both local and metastatic disease to discover whether treating the primary tumor with CAD12_PDL1 prior to systemic HER2.CAR T cell infusion affected both primary tumor and LN metastases.¹⁷ Combinatorial treatment improved both primary and metastatic tumor growth, whereas only the primary tumors were controlled in mice treated with CAD12_PDL1 alone. LN metastases of HNSCC tumors may express high levels of HER2,³³ and HER2.CAR T cells homed both to primary and metastasized tumors independent of CAD treatment but were insufficiently potent to control metastatic tumor growth. Only when HDAd-encoded transgenes were amplified during oncolysis of local tumor in the CAD system was there sufficient augmentation of HER2-CAR T for them to eliminate distant metastatic disease.

Overall, we demonstrate that local provision of different functional immunomodulatory molecules as a CAD package augments the antitumor effects of adoptively transferred CAR T cells and controls the growth of both bulky and metastasized tumors. Because intratumoral injection of adenoviruses has been tested in patients with a range of solid tumors,³⁴ our CAD concept could readily be applied to other solid tumors and used with CARs targeting different surface molecules.

MATERIALS AND METHODS

Adenoviral Vectors (HDAds and Onc.Ads)

HDAd without a transgene (HDAd0) was produced as described elsewhere.³⁵ HDAd containing the PD-L1-blocking antibody transgene driven by the cytomegalovirus (CMV) promoter (HDAdPD-L1) was produced as described elsewhere.⁷ Cytokine expression cassettes containing the cytokine transgene (IL-2, IL-7, IL-12p70, IL-15, or IL-21) driven by the EF1 promoter (HDAdCyto) were inserted into the pHDA28E4 vector. The IL-12p70 and PD-L1 mini-antibody expression cassettes were cloned into pHDA25E4. After confirmation of sequence and expression, all HDAds were rescued with chimeric helper virus 5/3 as described elsewhere.^{20,36} Onc.Ad5/3Δ24 plasmid DNA was a kind gift from Dr. David Curiel at Washington University,³⁷ and Onc.Ad5/3Δ24 was produced as described elsewhere.^{4,38}

Cell Lines

The human head and neck squamous cell carcinoma line FaDu and human triple negative breast cancer cell line MDA-MB468 were obtained from the ATCC (Manassas, VA) in 2016. The cell lines were authenticated utilizing short tandem repeat (STR) profiling by the ATCC. MDA-MB468 expressing human HER2 was produced as described elsewhere.³⁹ DHEP3 was a kind gift from Dr. Julio Aguirre-Ghiso at the Icahn School of Medicine at Mount Sinai. SCC-47, SCC-90, SCC-152, and SCC-154 were kind gifts from Dr. Susanne Gollin at the University of Pittsburgh. MDA686tu and MDA1586 were kind gifts from Dr. Jeffrey Myers at the M.D. Ander-

son Cancer Center. Cells were cultured under the recommended conditions.

Primary Cells

For the generation of CAR-modified T cells, we obtained peripheral blood from healthy donors through an institutional review board (IRB)-approved protocol at Baylor College of Medicine. Human peripheral blood mononuclear cells (PBMCs) were isolated using Ficoll-Paque Plus according to the manufacturer's instructions (Axis-Shield). The vector encoding the HER2-directed CAR incorporating the CD28 costimulatory endodomain (second-generation HER2.28ζ.CAR), the fusion protein EGFP-*ffLuc*, and the methodology for the production of retrovirus and CAR T cells have been described previously.¹⁴ Briefly, PBMCs were activated with OKT3 (1 mg/ml) (Ortho Biotech) and CD28 antibodies (1 mg/ml) (Becton Dickinson) and fed every 2 days with medium supplemented with 100 U/ml of recombinant human IL-2 (NIH). On day 3 post-OKT3/CD28 T blast generation, activated T cells (0.2×10^6 /ml) were added to an HER2.28ζ.CAR retrovirus-coated plate and centrifuged at $400 \times g$ for 5 min.

Co-culture Experiments

FaDu and SCC-47 cells genetically modified to express *ffLuc* were seeded in 12-well plates and infected with 100 vps per cell of HDAds as described in the figure legends. HER2.CAR T cells were added 24 hr post-infection at a 1:40 effector-to-target ratio and cultured for 5 additional days. Residual live cancer cells (*ffLuc* activity) were measured by plate reader (Life Technologies).

Flow Cytometry

The following monoclonal antibodies conjugated with fluorochrome were used: anti-human CD3, CD4, CD8, CD25, CD197, CD45RO, PD-1, TIM3, LAG3, PD-L1, phospho-STAT1 (Y701), phospho-STAT3 (Y705), phospho-STAT4 (Y693), phospho-STAT5 (Y694), recombinant human HER2-Fc chimera, and anti-Fc (for detection of HER2.CAR) (BD Biosciences, BioLegend, and R&D Systems). Cells were stained with these antibodies (Abs) for 30 min at 4°C. Live/dead discrimination was determined via inclusion of 7-aminoactinomycin D (7AAD; BD Pharmingen). Stained cells were analyzed using a Gallios flow cytometer with Kaluza software (BD Biosciences) according to the manufacturer's instructions.

Cytokine ELISA Assay

Forty thousand cells per well were seeded into 24-well plates. Cells were infected with HDAds or CAD (Onc.Ad:HDAd = 1:10) at the doses indicated in the figure legends and incubated at 37°C for 48 hr. Cytokine levels in media were measured using a BD cytokine multiplex bead assay according to the manufacturer's instructions (BD Biosciences).

MTS Assay

Ten thousand cells per well were seeded into 96-well plates. Cells were infected with Onc.Ad, HDAd, or CAD (Onc.Ad:HDAd, 1:10) at the doses indicated in the figure legends and incubated at 37°C for 96 hr. Cell viability was analyzed by MTS assay according to the

manufacturer's instruction (Promega). Cell viability was normalized to that of untreated cells.

Animal Experiments

All experiments involving mice were performed at Baylor College of Medicine in compliance and with approval from the Institutional Animal Care and Use Committee (IACUC). After counting, 1×10^6 harvested FaDu or SCC-47 cells were re-suspended in 100 μ L of PBS and subcutaneously injected into 5- to 6-week-old NSG male and female mice. After the tumor size reached 100 mm³, 1×10^8 vps of Onc.Ad, HDAd, or CAD (Onc.Ad:HDAd, 1:20; optimized ratio for animal experiments⁴) were intra-tumorally injected in a volume of 20 μ L. Three days after injection of Ads, mice received 1×10^6 HER2.CAR T cells intravenously. Tumor size was followed, and volumes were calculated using the formula width² \times length \times 0.5. To track the migration and survival of HER2.CAR T cells in vivo, T cells were genetically modified to express EGFP.ffLuc.⁷ Biodistribution of HER2.CAR T cells was assessed using an in vivo imaging system (Xenogen).⁷ For cytokine detection in serum samples, serum was collected at the times described in Results.

For the orthotopic model, 0.5×10^6 FaDu cells or *ffLuc*-expressing FaDu cells were re-suspended in a volume of 50 μ L of PBS and injected into the tongues of 5- to 6-week-old NSG female mice. Six days post-transplantation, a total of 1×10^8 vps of *CAd12_PDL1* (Onc.Ad:HDAd, 1:20) were injected in a volume of 20 μ L into the tongue. Three days after injection of Ads, mice received 1×10^6 HER2.CAR T cells intravenously. Tumors were assessed using an in vivo imaging system (Xenogen). Biodistribution of HER2.CAR T cells genetically modified to express EGFP.ffLuc was assessed using an in vivo imaging system (Xenogen).

Isolation of Tumor-Infiltrating HER2.CAR T Cells

After rinsing the collected tumors with PBS, the tumors were minced and incubated in RPMI medium containing collagenase type IV (5 mg/mL) and type I (1 mg/mL) (Thermo Fisher Scientific) at 37°C for 2 hr.⁴⁰ Cells were passed through a 70- μ m cell strainer (BD Pharmingen). Human T cells were isolated using Ficoll-Paque Plus according to the manufacturer's instructions (Axis-Shield) and stained with the described antibodies.

Quantification of HER2.CAR Copies at DNA and RNA Levels in Tumor-Infiltrating T Cells

HER2.CAR T cells were isolated from pooled tumors ($n = 4$) 22 days post-infusion and purified with a CD3 MACS column (Miltenyi Biotec). DNA and RNA were extracted from purified CD3⁺ cells as described elsewhere.⁴ HER2.CAR copies were quantified and normalized with human genomic glyceraldehyde 3-phosphate dehydrogenase (GAPDH; DNA samples) or human β -actin (RNA samples) (Table S1).

Quantification of Vector Genome DNA in Ad-Infected Cells

Cells were infected with 10 vps/cell of Onc.Ad, HDAd, or CAD (Onc.Ad:HDAd, 1:10) and harvested 48 hr post-infection. Tumors were injected with a total of 1×10^8 vps of Onc.Ad, HDAd, or CAD (Onc.Ad:HDAd, 1:20) and harvested at the indicated time points. Total

DNA was extracted from infected cells or tumors, and vector copies were quantified with primer sets (Table S1) as described elsewhere.⁷

Immunohistochemistry

Tongues and LN areas were collected from FaDu orthotopic mice 14 days post-injection of *CAd12_PDL1* and fixed in 10% neutral buffered formalin (Thermo Fisher Scientific). Paraffin-embedded tissues were stained with anti-human CD3 and p53 antibodies (Leica Biosystems) by the Human Tissue Acquisition and Pathology Core at Baylor College of Medicine.

Statistical Analysis

Data were analyzed by one-way ANOVA followed by Rank's protected least significant difference test (SigmaPlot).

SUPPLEMENTAL INFORMATION

Supplemental Information includes ten figures, one table, and one movie and can be found with this article online at <https://doi.org/10.1016/j.ymthe.2017.09.010>.

AUTHOR CONTRIBUTIONS

Conceptualization, M.S. and M.K.B.; Methodology, A.R.S., C.E.P., N.W., and K.T.; Investigation, A.R.S., C.E.P., N.W., K.T., and M.S.; Resources, A.S. and S.G.; Writing – Original Draft, A.R.S. and M.S.; Writing – Review & Editing, M.S. and M.K.B.; Supervision, M.S.; Funding Acquisition, A.R.S., S.G., M.K.B., and M.S.

CONFLICTS OF INTEREST

This research was supported by Tessa Therapeutics, Pte, Ltd.

ACKNOWLEDGMENTS

The authors would like to thank Catherine Gillespie in the Center for Cell and Gene Therapy at Baylor College of Medicine for editing the paper, Walter Mejia in the Center for Cell and Gene Therapy at Baylor College of Medicine for graphical design of the video abstract, and Dr. Brendan Lee in the Department of Molecular and Human Genetics at Baylor College of Medicine for support of the project. This work was supported by NIH grants R00HL098692 (to M.S.), T32HL092332 (to A.R.S.), and P30-CA125123 (to the Human Tissue Acquisition and Pathology Core) and a BCM Head and Neck seed grant and the Concern Foundation (to M.S.). This work was also supported by NIH grant P01 CA094237 (to M.K.B. and S.G.). K.T. was supported by the Strategic Young Researcher Overseas Visits Program for Accelerating Brain Circulation of the Japan Society for the Promotion of Science.

REFERENCES

1. Quail, D.F., and Joyce, J.A. (2013). Microenvironmental regulation of tumor progression and metastasis. *Nat. Med.* 19, 1423–1437.
2. Pardoll, D.M. (2012). The blockade of immune checkpoints in cancer immunotherapy. *Nat. Rev. Cancer* 12, 252–264.
3. Kershaw, M.H., Westwood, J.A., and Darcy, P.K. (2013). Gene-engineered T cells for cancer therapy. *Nat. Rev. Cancer* 13, 525–541.

4. Farzad, L., Cerullo, V., Yagyu, S., Bertin, T., Hemminki, A., Rooney, C., Lee, B., and Suzuki, M. (2014). Combinatorial treatment with oncolytic adenovirus and helper-dependent adenovirus augments adenoviral cancer gene therapy. *Mol. Ther. Oncolytics* 1, 14008.
5. Sharma, P., and Allison, J.P. (2015). Immune checkpoint targeting in cancer therapy: toward combination strategies with curative potential. *Cell* 161, 205–214.
6. Day, D., and Hansen, A.R. (2016). Immune-Related Adverse Events Associated with Immune Checkpoint Inhibitors. *BioDrugs* 30, 571–584.
7. Tanoue, K., Rosewell Shaw, A., Watanabe, N., Porter, C., Rana, B., Gottschalk, S., Brenner, M., and Suzuki, M. (2017). Armed oncolytic adenovirus expressing PD-L1 mini-body enhances antitumor effects of chimeric antigen receptor T cells in solid tumors. *Cancer Res.* 77, 2040–2051.
8. Khalil, D.N., Smith, E.L., Brentjens, R.J., and Wolchok, J.D. (2016). The future of cancer treatment: immunomodulation, CARs and combination immunotherapy. *Nat. Rev. Clin. Oncol.* 13, 394.
9. Yao, X., Ahmadzadeh, M., Lu, Y.C., Liewehr, D.J., Dudley, M.E., Liu, F., Schrupp, D.S., Steinberg, S.M., Rosenberg, S.A., and Robbins, P.F. (2012). Levels of peripheral CD4(+)FoxP3(+) regulatory T cells are negatively associated with clinical response to adoptive immunotherapy of human cancer. *Blood* 119, 5688–5696.
10. Liu, T.C., Galanis, E., and Kirn, D. (2007). Clinical trial results with oncolytic virotherapy: a century of promise, a decade of progress. *Nat. Clin. Pract. Oncol.* 4, 101–117.
11. Ferris, R.L. (2015). Immunology and Immunotherapy of Head and Neck Cancer. *J. Clin. Oncol.* 33, 3293–3304.
12. Seiwert, T.Y., Burtneis, B., Mehra, R., Weiss, J., Berger, R., Eder, J.P., Heath, K., McClanahan, T., Luncsford, J., Gause, C., et al. (2016). Safety and clinical activity of pembrolizumab for treatment of recurrent or metastatic squamous cell carcinoma of the head and neck (KEYNOTE-012): an open-label, multicentre, phase 1b trial. *Lancet Oncol.* 17, 956–965.
13. National Collaborating Centre for Cancer (UK). Melanoma: Assessment and Management. (NICE Guideline, No. 14). <https://www.ncbi.nlm.nih.gov/books/NBK315807/>.
14. Ahmed, N., Brawley, V.S., Hegde, M., Robertson, C., Ghazi, A., Gerken, C., Liu, E., Dakhova, O., Ashoori, A., Corder, A., et al. (2015). Human Epidermal Growth Factor Receptor 2 (HER2) -Specific Chimeric Antigen Receptor-Modified T Cells for the Immunotherapy of HER2-Positive Sarcoma. *J. Clin. Oncol.* 33, 1688–1696.
15. Ahmed, N., Brawley, V., Hegde, M., Bielamowicz, K., Kalra, M., Landi, D., Robertson, C., Gray, T.L., Diouf, O., Wakefield, A., et al. (2017). HER2-Specific Chimeric Antigen Receptor-Modified Virus-Specific T Cells for Progressive Glioblastoma: A Phase I Dose-Escalation Trial. *JAMA Oncol.* 3, 1094–1101.
16. Pollock, N.I., and Grandis, J.R. (2015). HER2 as a therapeutic target in head and neck squamous cell carcinoma. *Clin. Cancer Res.* 21, 526–533.
17. Leemans, C.R., Braakhuis, B.J., and Brakenhoff, R.H. (2011). The molecular biology of head and neck cancer. *Nat. Rev. Cancer* 11, 9–22.
18. Markley, J.C., and Sadelain, M. (2010). IL-7 and IL-21 are superior to IL-2 and IL-15 in promoting human T cell-mediated rejection of systemic lymphoma in immunodeficient mice. *Blood* 115, 3508–3519.
19. Pegram, H.J., Lee, J.C., Hayman, E.G., Imperato, G.H., Tedder, T.F., Sadelain, M., and Brentjens, R.J. (2012). Tumor-targeted T cells modified to secrete IL-12 eradicate systemic tumors without need for prior conditioning. *Blood* 119, 4133–4141.
20. Suzuki, M., Cela, R., Clarke, C., Bertin, T.K., Mourinho, S., and Lee, B. (2010). Large-scale production of high-quality helper-dependent adenoviral vectors using adherent cells in cell factories. *Hum. Gene Ther.* 21, 120–126.
21. Leonard, W.J., and Spolski, R. (2005). Interleukin-21: a modulator of lymphoid proliferation, apoptosis and differentiation. *Nat. Rev. Immunol.* 5, 688–698.
22. Teng, M.W., Bowman, E.P., McElwee, J.J., Smyth, M.J., Casanova, J.L., Cooper, A.M., and Cua, D.J. (2015). IL-12 and IL-23 cytokines: from discovery to targeted therapies for immune-mediated inflammatory diseases. *Nat. Med.* 21, 719–729.
23. Taipale, K., Liikainen, I., Koski, A., Heiskanen, R., Kanerva, A., Hemminki, O., Oksanen, M., Grönberg-Vähä-Koskela, S., Hemminki, K., Joensuu, T., and Hemminki, A. (2016). Predictive and prognostic clinical variables in cancer patients treated with adenoviral oncolytic immunotherapy. *Mol. Ther.* 24, 1323–1332.
24. Parkin, D.M., Bray, F., Ferlay, J., and Pisani, P. (2005). Global cancer statistics, 2002. *CA Cancer J. Clin.* 55, 74–108.
25. Lin, L.T., Chang, C.Y., Chang, C.H., Wang, H.E., Chiou, S.H., Liu, R.S., Lee, T.W., and Lee, Y.J. (2016). Involvement of let-7 microRNA for the therapeutic effects of Rhenium-188-embedded liposomal nanoparticles on orthotopic human head and neck cancer model. *Oncotarget* 7, 65782–65796.
26. Sweeny, L., Hartman, Y.E., Zinn, K.R., Prudent, J.R., Marshall, D.J., Shekhani, M.S., and Rosenthal, E.L. (2013). A novel extracellular drug conjugate significantly inhibits head and neck squamous cell carcinoma. *Oral Oncol.* 49, 991–997.
27. Xu, X.J., Song, D.G., Poussin, M., Ye, Q., Sharma, P., Rodríguez-García, A., Tang, Y.M., and Powell, D.J. (2016). Multiparameter comparative analysis reveals differential impacts of various cytokines on CART cell phenotype and function ex vivo and in vivo. *Oncotarget* 7, 82354–82368.
28. Xu, Y., Zhang, M., Ramos, C.A., Durett, A., Liu, E., Dakhova, O., Liu, H., Creighton, C.J., Gee, A.P., Heslop, H.E., et al. (2014). Closely related T-memory stem cells correlate with in vivo expansion of CAR-CD19-T cells and are preserved by IL-7 and IL-15. *Blood* 123, 3750–3759.
29. Pegram, H.J., Purdon, T.J., van Leeuwen, D.G., Curran, K.J., Giralt, S.A., Barker, J.N., and Brentjens, R.J. (2015). IL-12-secreting CD19-targeted cord blood-derived T cells for the immunotherapy of B-cell acute lymphoblastic leukemia. *Leukemia* 29, 415–422.
30. DuPage, M., and Bluestone, J.A. (2016). Harnessing the plasticity of CD4(+) T cells to treat immune-mediated disease. *Nat. Rev. Immunol.* 16, 149–163.
31. Atkins, M.B., Robertson, M.J., Gordon, M., Lotze, M.T., DeCoste, M., DuBois, J.S., Ritz, J., Sandler, A.B., Edington, H.D., Garzone, P.D., et al. (1997). Phase I evaluation of intravenous recombinant human interleukin 12 in patients with advanced malignancies. *Clin. Cancer Res.* 3, 409–417.
32. Nishio, N., Diaconu, I., Liu, H., Cerullo, V., Caruana, I., Hoyos, V., Bouchier-Hayes, L., Savoldo, B., and Dotti, G. (2014). Armed oncolytic virus enhances immune functions of chimeric antigen receptor-modified T cells in solid tumors. *Cancer Res.* 74, 5195–5205.
33. Masuelli, L., Budillon, A., Marzocchella, L., Mrozek, M.A., Vitolo, D., Di Gennaro, E., Losito, S., Sale, P., Longo, F., Ionna, F., et al. (2012). Caveolin-1 overexpression is associated with simultaneous abnormal expression of the E-cadherin/ α - β catenins complex and multiple ErbB receptors and with lymph nodes metastasis in head and neck squamous cell carcinomas. *J. Cell. Physiol.* 227, 3344–3353.
34. Kanerva, A., Nikisalmi, P., Diaconu, I., Koski, A., Cerullo, V., Liikainen, I., Tähtinen, S., Oksanen, M., Heiskanen, R., Pesonen, S., et al. (2013). Antiviral and antitumor T-cell immunity in patients treated with GM-CSF-coding oncolytic adenovirus. *Clin. Cancer Res.* 19, 2734–2744.
35. Suzuki, M., Bertin, T.K., Rogers, G.L., Cela, R.G., Zolotukhin, I., Palmer, D.J., Ng, P., Herzog, R.W., and Lee, B. (2013). Differential type I interferon-dependent transgene silencing of helper-dependent adenoviral vs. adeno-associated viral vectors in vivo. *Mol. Ther.* 21, 796–805.
36. Guse, K., Suzuki, M., Sule, G., Bertin, T.K., Tyynismaa, H., Ahola-Erkkilä, S., Palmer, D., Suomalainen, A., Ng, P., Cerullo, V., et al. (2012). Capsid-modified adenoviral vectors for improved muscle-directed gene therapy. *Hum. Gene Ther.* 23, 1065–1070.
37. Kanerva, A., Zinn, K.R., Chaudhuri, T.R., Lam, J.T., Suzuki, K., Uil, T.G., Hakkarainen, T., Bauerschmitz, G.J., Wang, M., Liu, B., et al. (2003). Enhanced therapeutic efficacy for ovarian cancer with a serotype 3 receptor-targeted oncolytic adenovirus. *Mol. Ther.* 8, 449–458.
38. Fueyo, J., Gomez-Manzano, C., Alemany, R., Lee, P.S., McDonnell, T.J., Mitlianga, P., Shi, Y.X., Levin, V.A., Yung, W.K., and Kyritsis, A.P. (2000). A mutant oncolytic adenovirus targeting the Rb pathway produces anti-glioma effect in vivo. *Oncogene* 19, 2–12.
39. Mata, M., Vera, J.F., Gerken, C., Rooney, C.M., Miller, T., Pfent, C., Wang, L.L., Wilson-Robles, H.M., and Gottschalk, S. (2014). Toward immunotherapy with redirected T cells in a large animal model: ex vivo activation, expansion, and genetic modification of canine T cells. *J. Immunother.* 37, 407–415.
40. Kim, M.P., Evans, D.B., Wang, H., Abbruzzese, J.L., Fleming, J.B., and Gallick, G.E. (2009). Generation of orthotopic and heterotopic human pancreatic cancer xenografts in immunodeficient mice. *Nat. Protoc.* 4, 1670–1680.

YMTHE, Volume 25

Supplemental Information

Adenovirotherapy Delivering Cytokine and Checkpoint Inhibitor Augments CAR T Cells against Metastatic Head and Neck Cancer

Amanda Rosewell Shaw, Caroline E. Porter, Norihiro Watanabe, Kiyonori Tanoue, Andrew Sikora, Stephen Gottschalk, Malcolm K. Brenner, and Masataka Suzuki

Supplemental Table 1. *Primer sequences.*

Supplemental Fig. 1. *HNSCC lines heterogeneously express HER2.* HER2 expression was analyzed by flow cytometry on both HPV negative and HPV positive HNSCC lines. Triple negative breast cancer cell line MDA-MB-468, and MDA-expressing human HER2 (MDAHER2) were used as controls.

Supplemental Fig. 2. *HER2.CAR T-cells have minimal expansion in NSG mice without tumors.* A total of 1×10^6 *ffLuc*-expressing HER2.CAR T-cells were systemically administered to NSG mice. Control mice received vehicle alone. Bioluminescence of HER2.CAR T-cells was monitored at different time points. Data are presented as means \pm SD (n=5).

Supplemental Fig. 3. *Both HNSCC lines induce PD-L1 expression in the presence of IFN γ , and HDAdCyto and PD-L1 blocking antibody increase the anti-tumor efficacy of HER2.CAR T-cells in vitro.* (A) FaDu and SCC47 were cultured in the presence or absence of 10 ng/mL recombinant IFN γ . Cells were harvested at 24 hours, and the expression of PD-L1 was analyzed by flow cytometry. (B) SCC-47 or FaDu expressing *ffLuc* cells were co-infected with 100 vp/cell of HDAdCyto and HDAdPD-L1. HER2.CAR T-cells were added at 24 hours post-infection (effector:target ratio of 1:40). Cells were harvested 120 hours post-co-culture, and viable cancer cells were analyzed by luciferase assay. Data are presented as means \pm SD (n=4). * $P < 0.001$. The experiments were repeated with HER2.CAR T-cells derived from a second donor with similar results.

Supplemental Fig. 4. *Phenotype of HER2.CAR T-cells.* (A) Before infusion to mice, HER2.CAR expression, CD4 and CD8 ratio, memory phenotype and PD-1 expression of HER2.CAR T-cells were analyzed by flow cytometry. (B) T-cells were isolated from tumor sites at 22 days post-infusion, and CD4 and CD8 ratio, memory phenotype and PD-1, TIM3, LAG3 expression were analyzed by flow cytometry. The experiments were repeated with similar results.

Supplemental Fig. 5. *HNSCC lines resist Onc.Ad in vivo.* FaDu and SCC-47 cells were transplanted into the right flanks of NSG mice (pink: female, blue: male). A total of 1×10^8 vp Onc.Ads were intra-tumorally injected. Tumor volumes were measured at different time points. Kaplan-Meier survival curve after injection of Onc.Ads. The end point was established as tumor volume of $> 1,500 \text{ mm}^3$. Data are presented as means \pm SD (n=8-9). * $P=0.04$.

Supplemental Fig. 6. *Tumor-infiltrating HER2. CAR T-cells were detected at tumor sites overtime.* A total of 1×10^8 vp of Onc.Ad, CAdPDL1, CAdIL-12 or CAdI2_PDL1 (Onc:HD=1:20) were injected intra-tumorally. A total of 1×10^6 HER2.CAR T-cells expressing firefly luciferase (*ffLuc*) were systemically administered 3 days post-injection of Ads. Bioluminescence of HER2.CAR T-cells was monitored at different time points.

Supplemental Fig. 7. *Tumor-infiltrating HER2. CAR T-cells maintain HER2.CAR expression at 105 days post-injection.* T-cells were isolated from tumor sites at 105 days post-infusion, and HER2.CAR expression were analyzed by flow cytometry. The experiments were repeated with similar results.

Supplemental Fig. 8. *Combinatorial treatments did not cause weight loss in mice.* FaDu or SCC-47 cells were transplanted into the right flanks of NSG mice. A total of 1×10^8 vp of Onc.Ad, CAdPDL1, CAdIL-12 or CAdI2_PDL1 (Onc:HD=1:20) were injected intra-tumorally. A total of 1×10^6 HER2.CAR T-cells were systemically administered 3 days post-injection of Ads. Body weights were measured at different time points. Data are presented as means \pm SD (n=8-10).

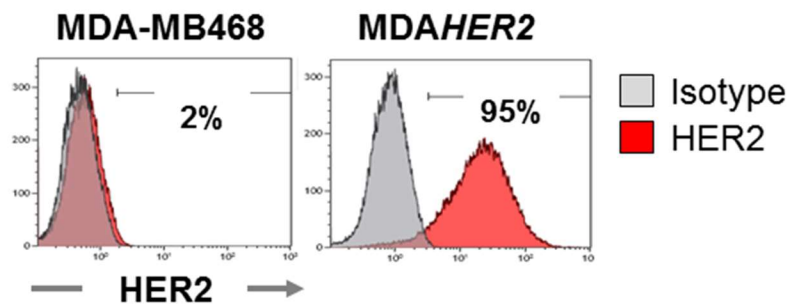
Supplemental Fig. 9. *HER2.CAR T-cells home both primary and metastasized tumors in FaDu orthotopic mice.* FaDu cells were transplanted into the tongues of NSG mice. A total of 1×10^8 vp of CAdI2_PDL1 (Onc:HD=1:20) were injected into the tongue. A total of 1×10^6 HER2.CAR T-cells were systemically administered 3 days post-injection of CAd. **(A)** Tongue and lymph node area were collected at 14 days post-injection of CAd and fixed. Paraffin sections were stained with H&E, anti-human CD3 and anti-human p53 antibodies. **(B)** Total DNA was extracted from tongue and lymph node area at 14 days post-injection of CAd, and HER2.CAR, Onc.Ad and HDAd copy

numbers in each tissue were quantified. After normalization of each copy number with mouse genomic GAPDH, copy numbers of tissue treated with *CAd12_PDL1* and HER2.CAR T-cells were normalized with that of control mice. Data are presented (n=2).

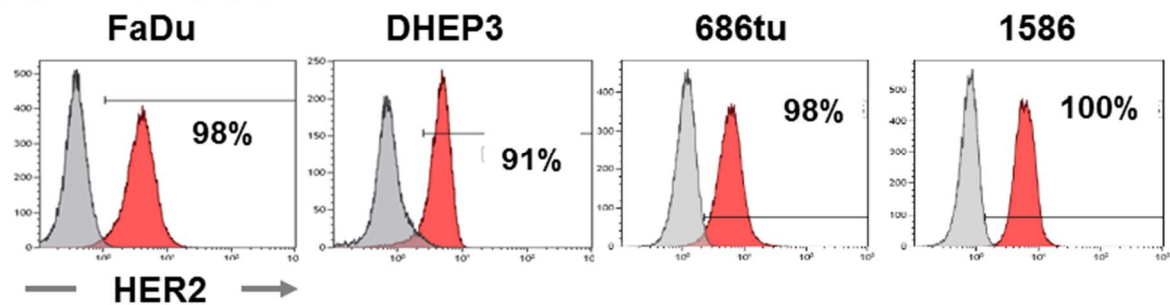
Supplemental Fig. 10. *Combinatorial treatments did not cause weight loss due to tumor growth in HNSCC orthotopic mice.* FaDu cells were transplanted into the tongues of NSG mice. A total of 1×10^8 vp of *CAd12_PDL1* (Onc:HD=1:20) were injected into the tongue. A total of 1×10^6 HER2.CAR T-cells expressing *ffLuc* were systemically administered 3 days post-injection of CAd. Body weights were measured at different time points. Data are presented as means \pm SD (n=6).

Primer name	Sequence
E1A (Onc.Ad)	5'-TCCGGTTTCTATGCCAAACCT-3' 5'-TCCTCCGGTGATAATGACAAGA-3'
Stuffer (HDAd)	5'-TCTGAATAATTTTGTGTTACTCATAGCGCG-3' 5'-CCCATAAGCTCCTTTTAACTTGTTAAAGTC-3'
HER2.CAR (CAR T-cell)	5'-GAGGTACAACCTGCAGCAGTCTGGA-3' 5'-TTCCAAAGAGAAGTCAAACCGTCC-3'
Human genomic GAPDH	5'-CATGCCTTCTTGCCTCTTGTCTCTTAGAT-3' 5'-CCATGGGTGGAATCATATTGGAACATGTAA-3'
Mouse genomic GAPDH	5'-TAGGCCAGGATGTAAAGGTCATTAAG-3' 5'-CCAGAAAGGTCACACGGCTAAA-3'
Human β -actin	5'-GCCAACCGCGAGAAGATGACC-3' 5'-CTCCTTAATGTCACGCACGATTTC-3'

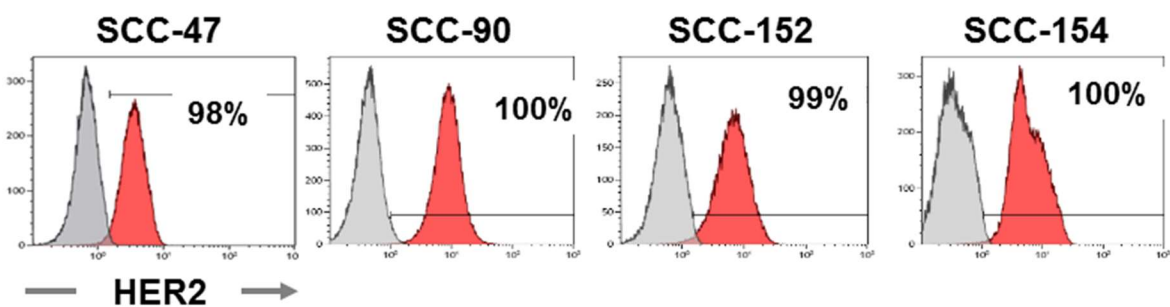
Supplemental Figure 1



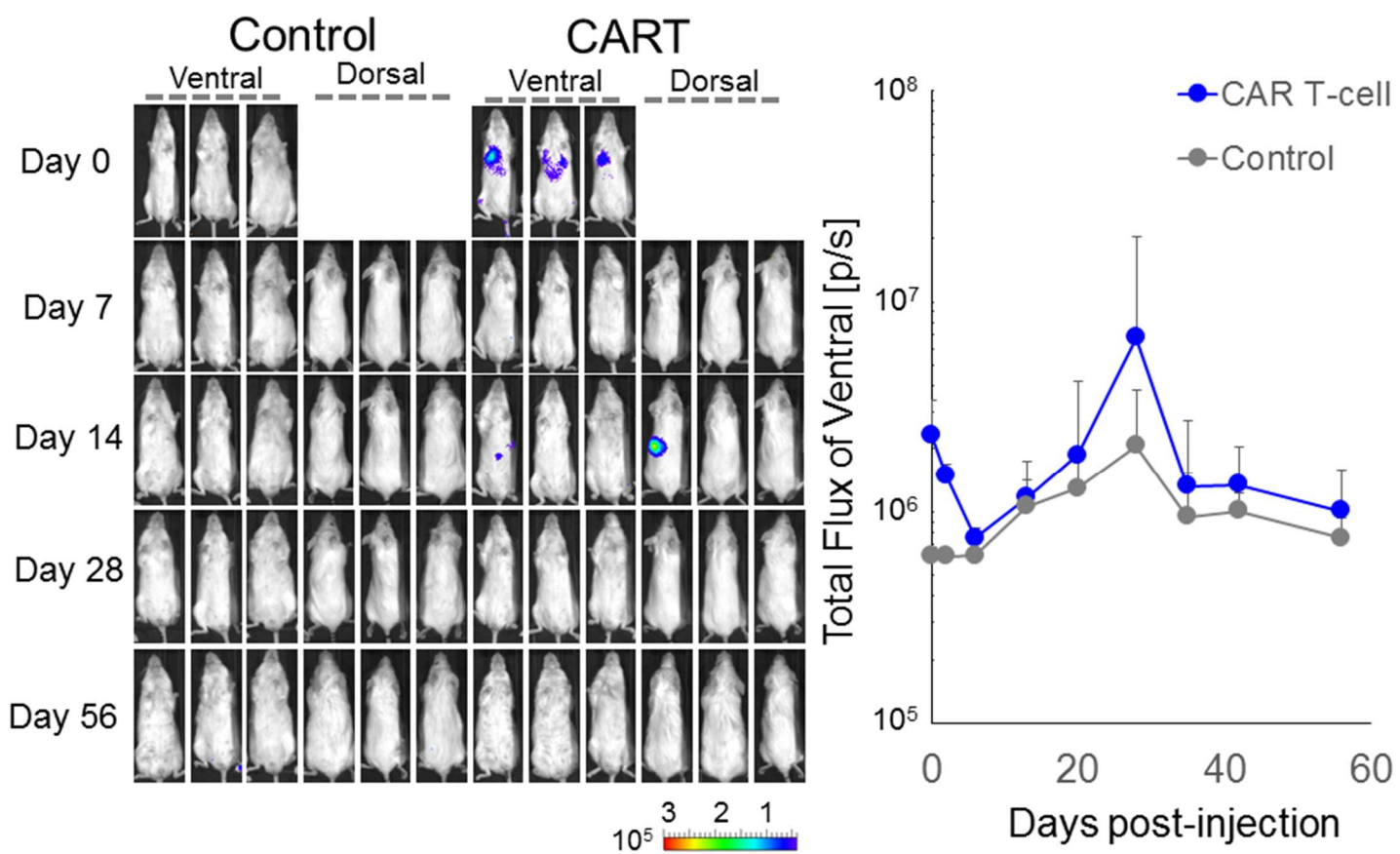
❖ HPV- HNSCC



❖ HPV+ HNSCC

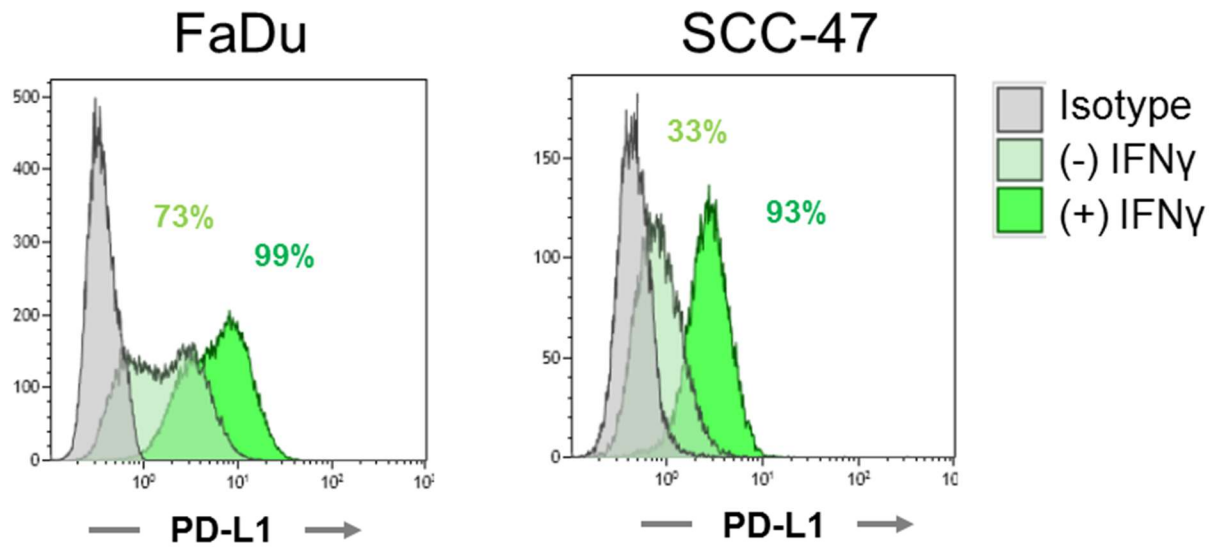


Supplemental Figure 2



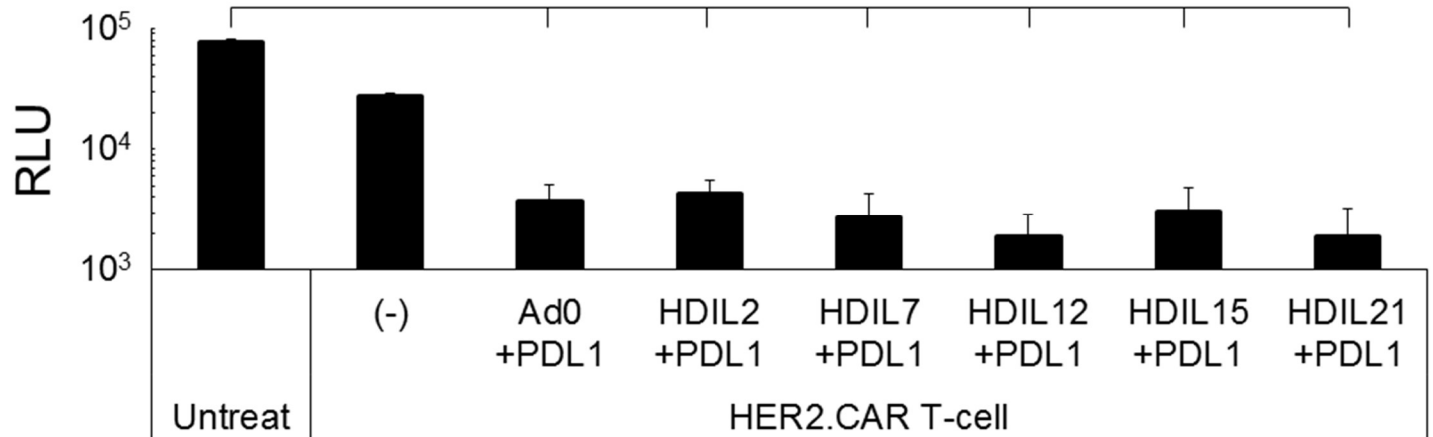
Supplemental Figure 3

A

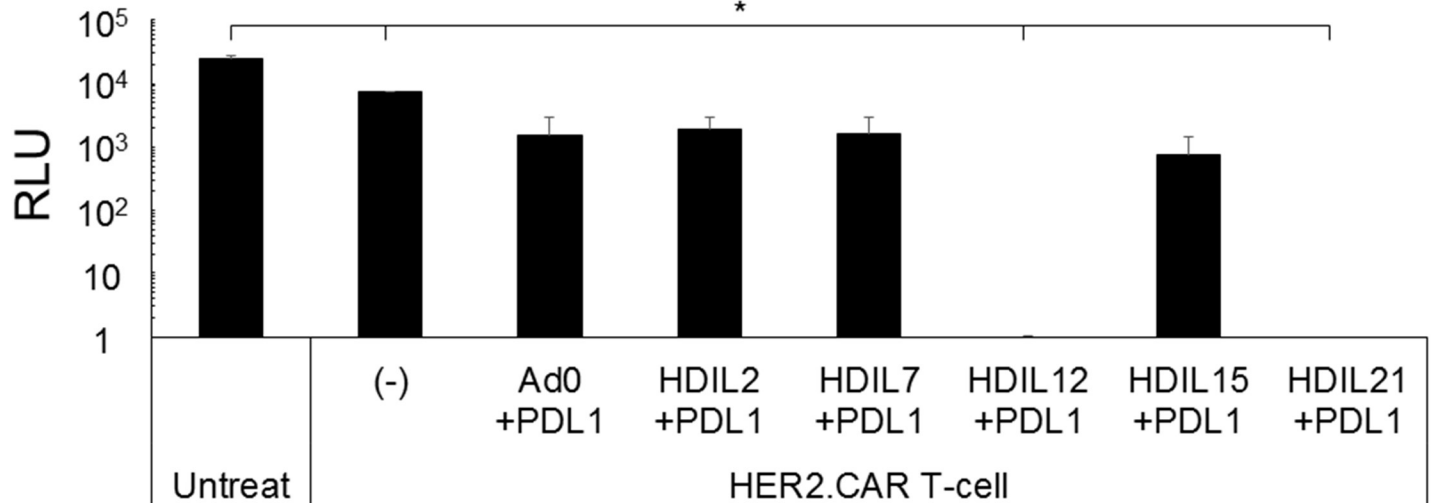


B

❖ FaDu



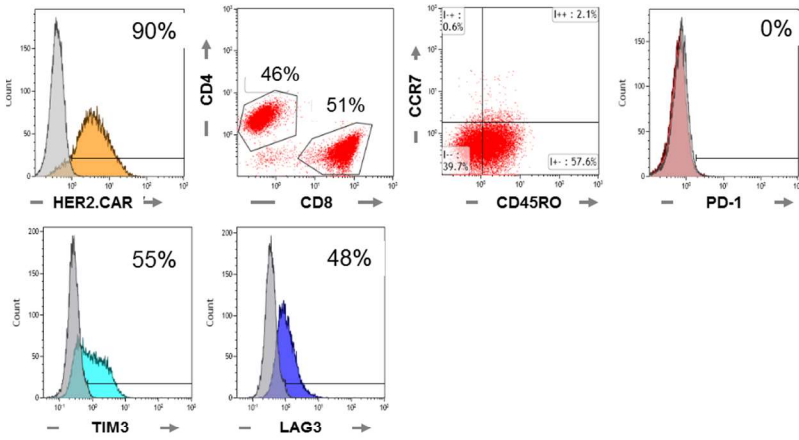
❖ SCC47



Supplemental Figure 4

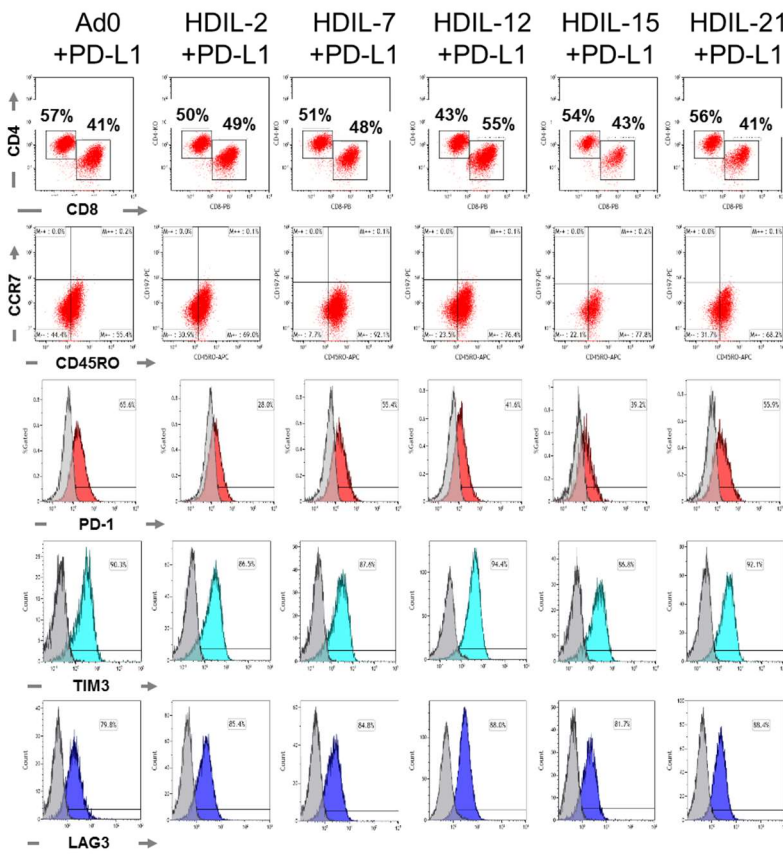
A

❖ Pre-infusion

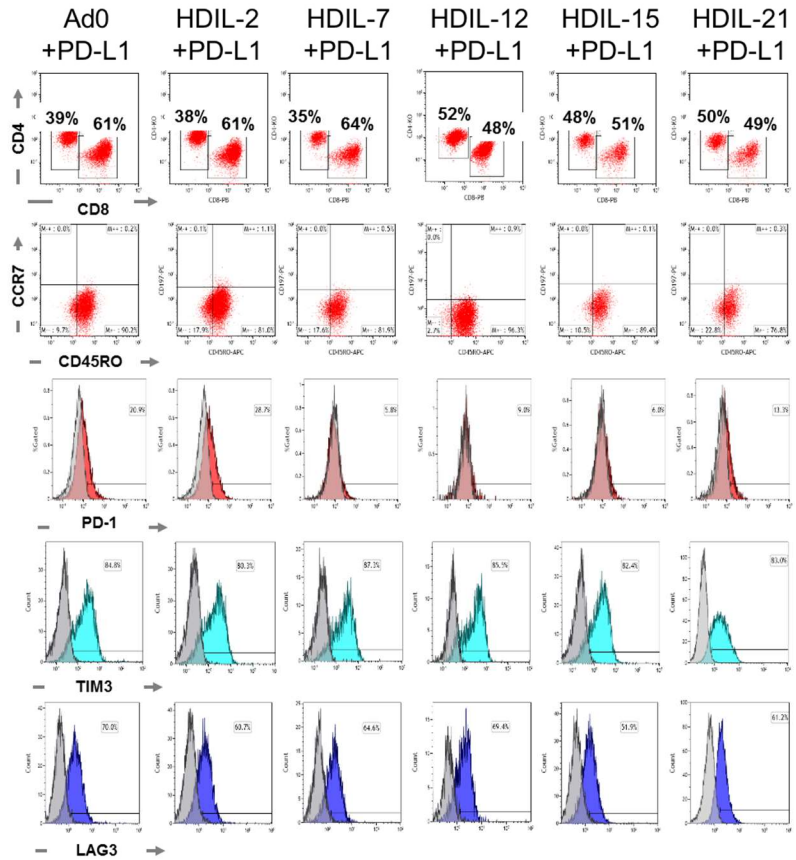


B

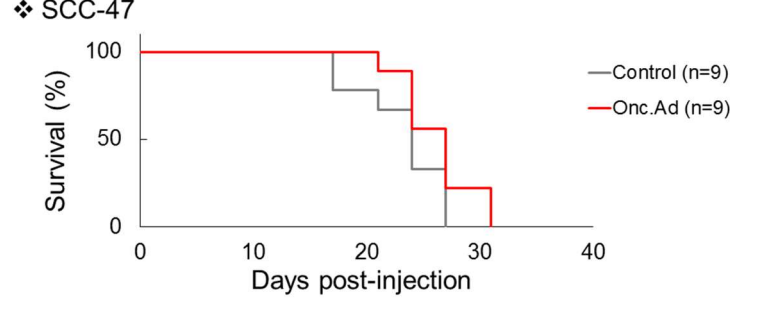
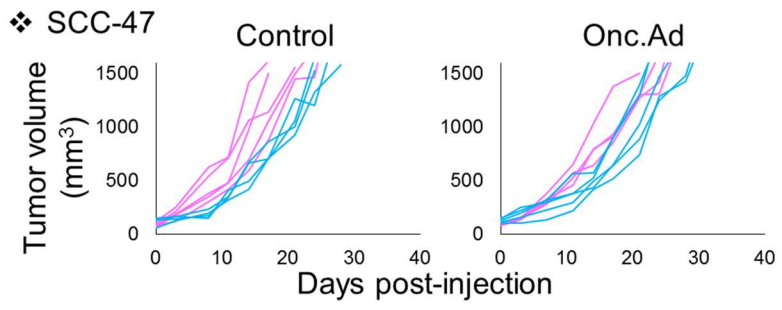
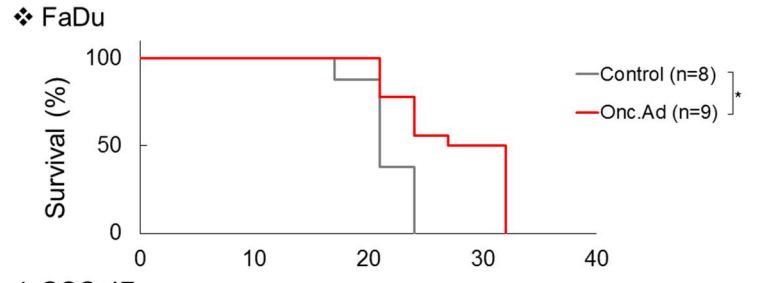
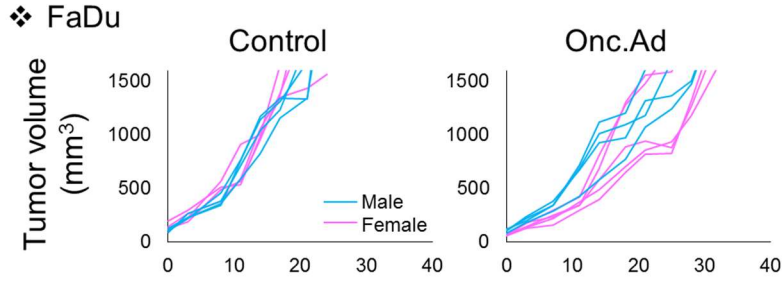
❖ FaDu



❖ SCC47

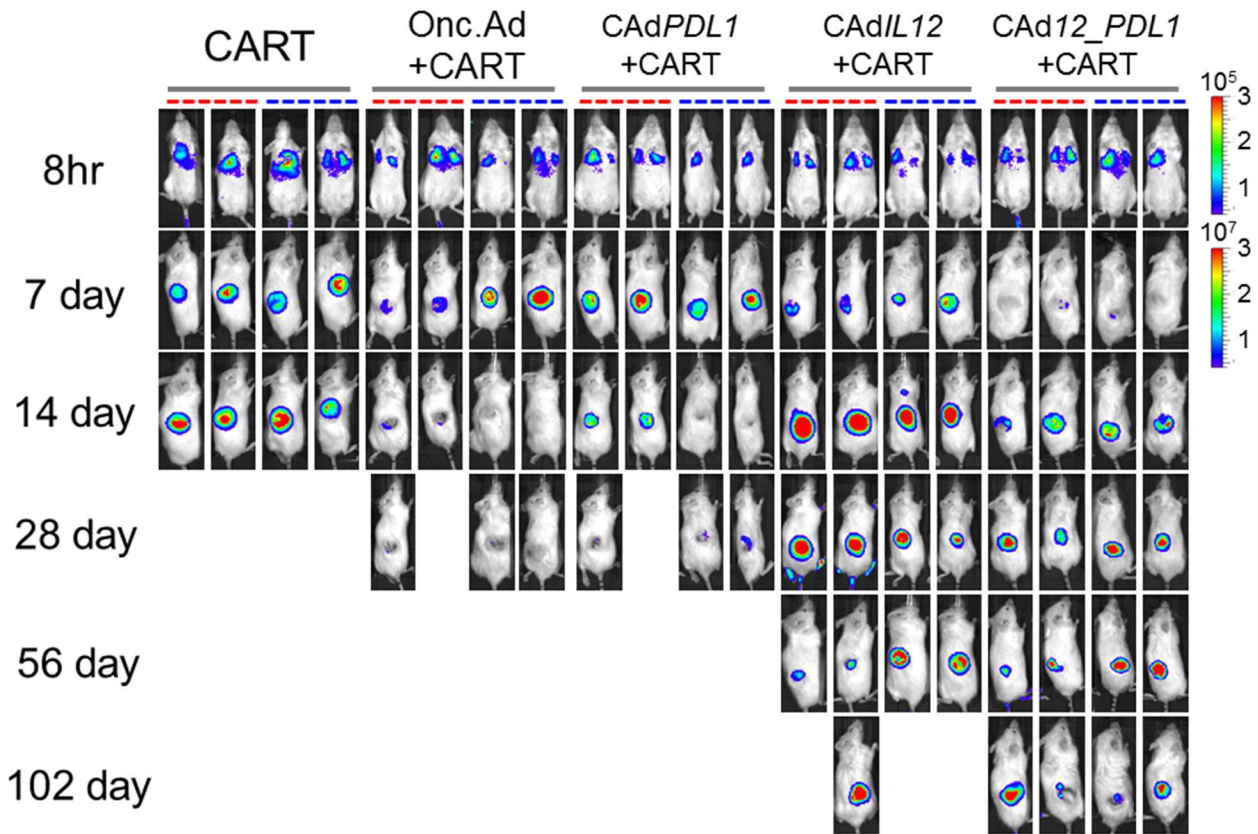


Supplemental Figure 5

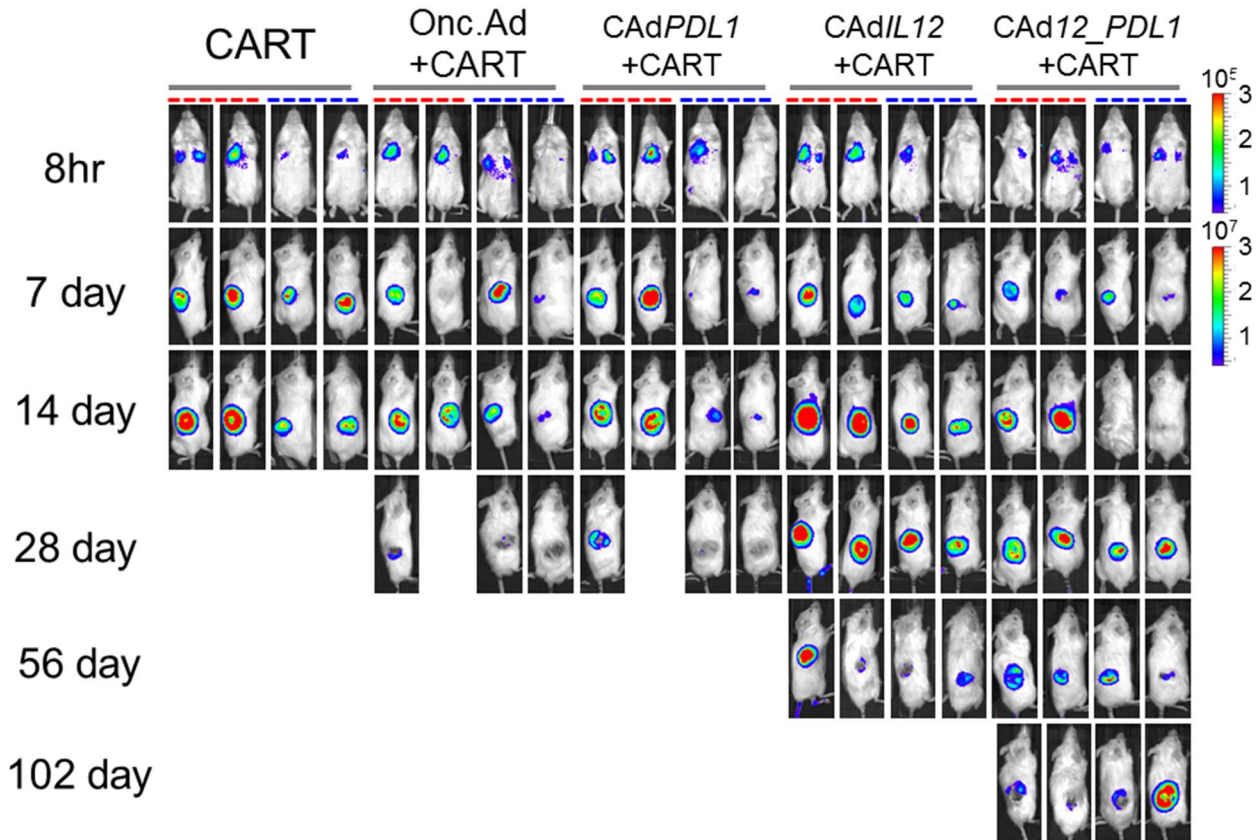


Supplemental Figure 6

❖ FaDu

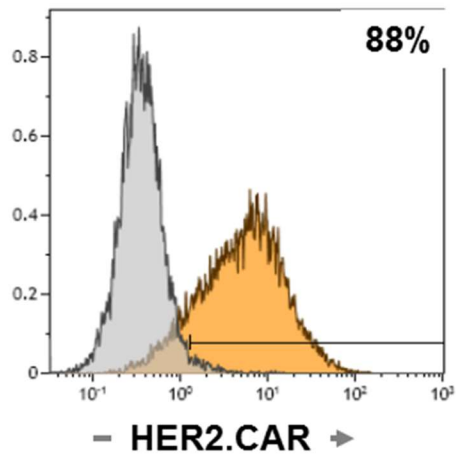


❖ SCC-47

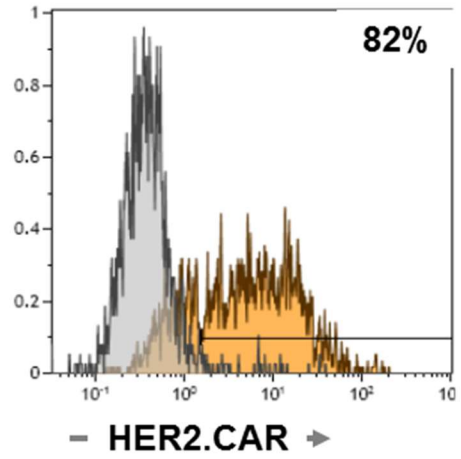


Supplemental Figure 7

❖ FaDu TIL: 105 day

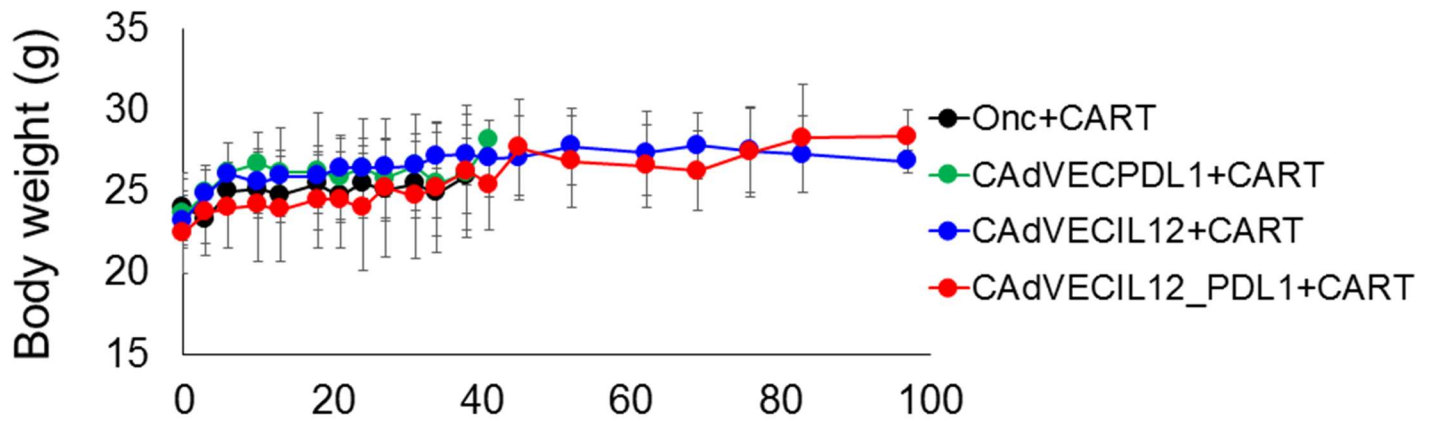


❖ SCC-47 TIL: 105 day

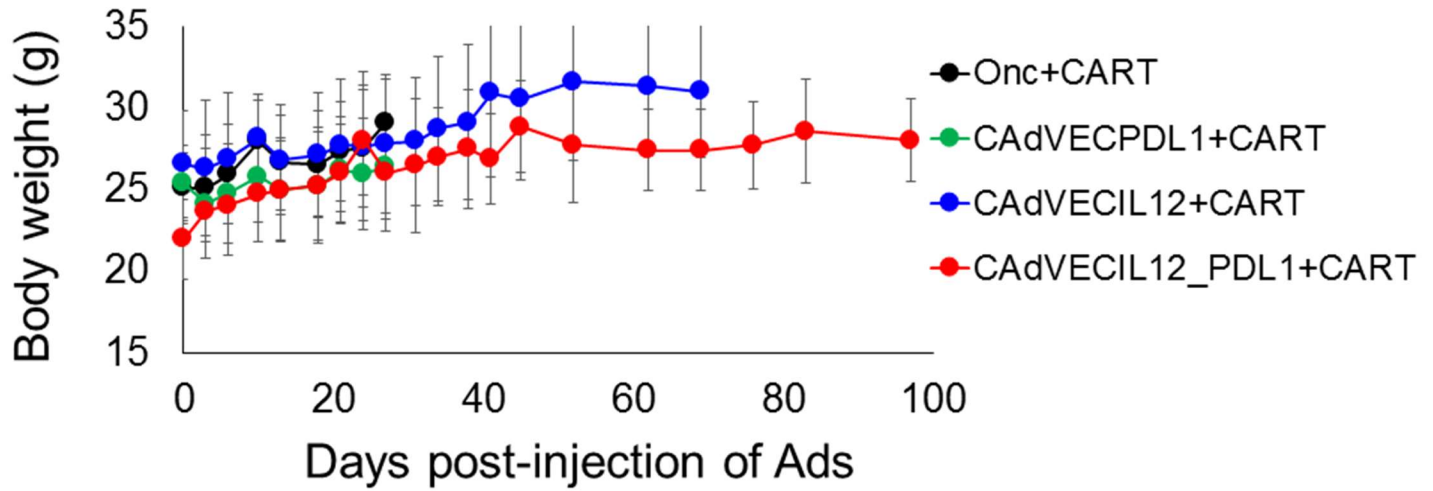


Supplemental Figure 8

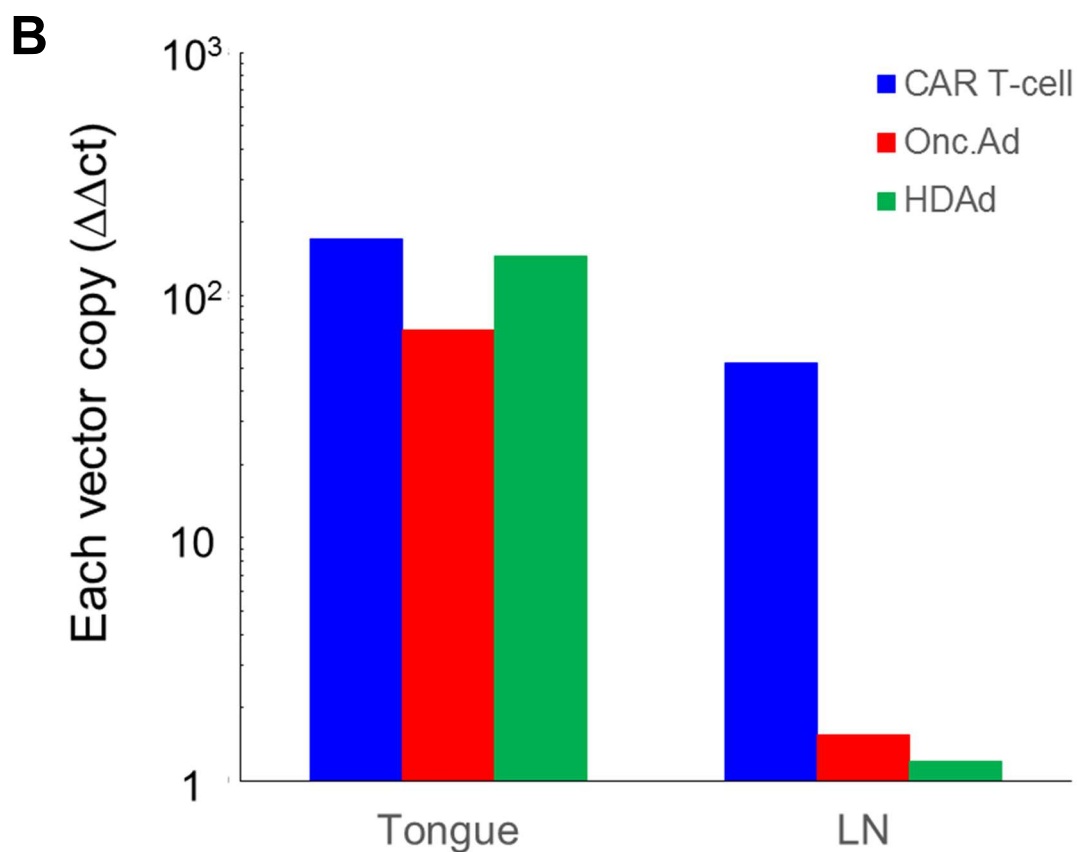
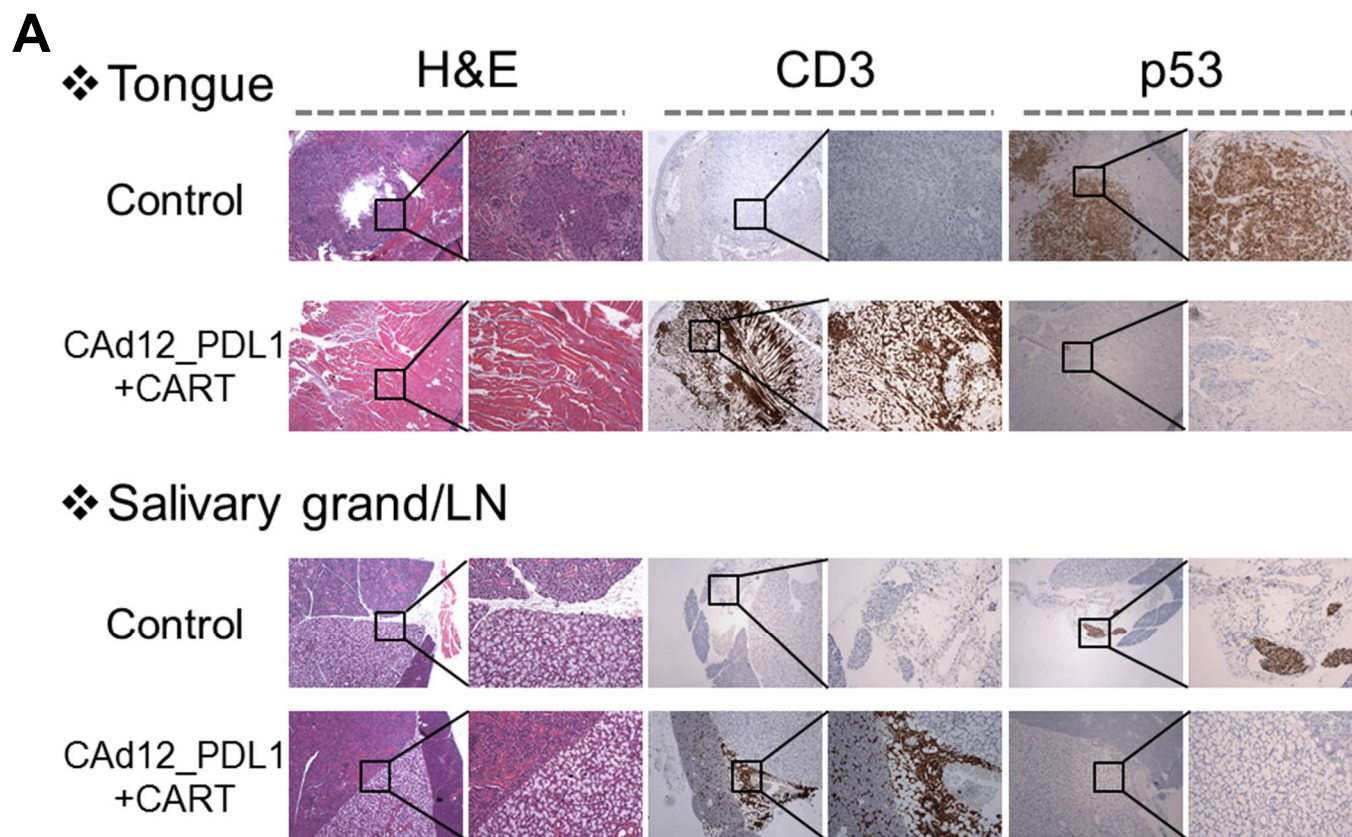
❖ FaDu



❖ SCC-47



Supplemental Figure 9



Supplemental Figure 10

